Cell

Article

Primate hemorrhagic fever-causing arteriviruses are poised for spillover to humans

Graphical abstract

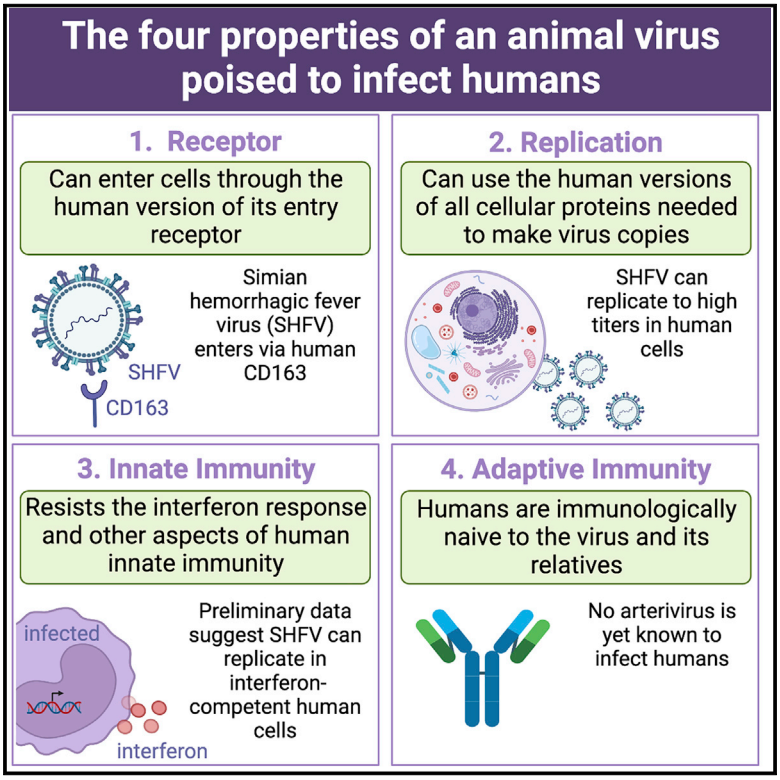

Highlights

- SHFV uses an intracellular receptor, CD163, for cellular entry
- CD163 divergence in primates of some species poses a barrier to SHFV entry
- All cellular proteins required for SHFV replication are functional in human cells
- SHFV replication in human cells suggests potential for zoonotic transmission

Authors

Cody J. Warren, Shuiqing Yu, Douglas K. Peters, ..., Tony L. Goldberg, Jens H. Kuhn, Sara L. Sawyer

Correspondence

kuhnjens@mail.nih.gov (J.H.K.), ssawyer@colorado.edu (S.L.S.)

In brief

Arteriviruses that infect nonhuman primates can cause fatal hemorrhagic fevers. One such virus, SHFV, is capable of infecting and replicating in human monocytes by using CD163 as the intracellular receptor. This suggests that SHFV may not require major adaptations for the human host, and that surveillance is needed for this virus family.

Warren et al., 2022, Cell *185*, 1–12
October 13, 2022
https://doi.org/10.1016/j.cell.2022.09.022

CellPress

Cell

CellPress

Article

Primate hemorrhagic fever-causing arteriviruses are poised for spillover to humans

Cody J. Warren,[1,5] Shuiqing Yu,[2] Douglas K. Peters,[1,6] Arturo Barbachano-Guerrero,[1] Qing Yang,[1,7] Bridget L. Burris,[3] Gabriella Worwa,[2] I-Chueh Huang,[2,8] Gregory K. Wilkerson,[3,9] Tony L. Goldberg,[4] Jens H. Kuhn,[2,*] and Sara L. Sawyer[1,10,*]

[1]BioFrontiers Institute, Department of Molecular, Cellular, and Developmental Biology, University of Colorado, Boulder, CO 80303, USA
[2]Integrated Research Facility at Fort Detrick, National Institute of Allergy and Infectious Diseases, National Institutes of Health, Fort Detrick, Frederick, MD 21702, USA
[3]Department of Comparative Medicine, Michale E. Keeling Center for Comparative Medicine and Research, The University of Texas MD Anderson Cancer Center, Bastrop, TX 78602, USA
[4]Department of Pathobiological Sciences, University of Wisconsin–Madison, Madison, WI 53706, USA
[5]Present address: Department of Veterinary Biosciences, The Ohio State University, Columbus, OH 43210, USA
[6]Present address: Inotiv, Boulder, CO 80301, USA
[7]Present address: Vaccine and Infectious Disease Division, Fred Hutchinson Cancer Center, Seattle, WA 98109, USA
[8]Present address: Janssen Research & Development, Johnson & Johnson, Brisbane, CA 94005, USA
[9]Present address: Department of Clinical Sciences, North Carolina State University, Raleigh, NC 27607, USA
[10]Lead contact
*Correspondence: kuhnjens@mail.nih.gov (J.H.K.), ssawyer@colorado.edu (S.L.S.)
https://doi.org/10.1016/j.cell.2022.09.022

SUMMARY

Simian arteriviruses are endemic in some African primates and can cause fatal hemorrhagic fevers when they cross into primate hosts of new species. We find that CD163 acts as an intracellular receptor for simian hemorrhagic fever virus (SHFV; a simian arterivirus), a rare mode of virus entry that is shared with other hemorrhagic fever-causing viruses (e.g., Ebola and Lassa viruses). Further, SHFV enters and replicates in human monocytes, indicating full functionality of all of the human cellular proteins required for viral replication. Thus, simian arteriviruses in nature may not require major adaptations to the human host. Given that at least three distinct simian arteriviruses have caused fatal infections in captive macaques after host-switching, and that humans are immunologically naive to this family of viruses, development of serology tests for human surveillance should be a priority.

INTRODUCTION

Simian hemorrhagic fever is a lethal disease that has been documented in captive Asian macaques (*Macaca* spp.). Outbreaks have occurred in macaque colonies worldwide (Figure 1A) and have been traced to at least three different simian viruses (Figure 1B, in red) classified in subfamily *Simarterivirinae* (*Nidovirales*: *Arteriviridae*) (Kuhn et al., 2016; Lauck et al., 2015). These simian arteriviruses likely entered primate facilities through the import of subclinically infected wild African monkeys. To date, primate facilities remain vigilant about preventing exposure to these viruses (Johnson et al., 2011; Lauck et al., 2015). Human infections at affected primate facilities have not been detected. Further, there is no way to surveil for prior human exposure in Africa, where these viruses are endemic in primates, because no serology tests exist. In the absence of strong biological indications that humans could be at risk of infection with these viruses, there has been little impetus to interrogate the interface between nonhuman primates and humans in Africa to exclude cryptic spillover events or subclinical infection cycles.

Although the natural primate reservoirs of these viruses remain poorly understood, recent discovery efforts have identified broad arterivirus diversity in apparently healthy African monkeys of numerous species ranging across Africa (Figure 1C) (Bailey et al., 2014a, 2014b, 2016). Infected monkeys can carry high viral loads (Bailey et al., 2016). In some locations, primates of these species interact with people in direct and often aggressive ways, leading to high risk of exposure for humans. For instance, red colobus monkeys in western Uganda are infected with high viral loads of two simian arteriviruses (Lauck et al., 2013) and are known to bite and scratch local people (Paige et al., 2014, 2017). Such human-primate antagonism is widespread and increasing across Africa (Hill, 2018; Hockings, 2016).

The recent finding that arteriviruses can replicate in primary ape (chimpanzee and gorilla) cells (Cai et al., 2021) evokes parallels to simian immunodeficiency virus (SIV; *Retroviridae*). SIV first crossed from African monkeys into apes, a key "stepping-stone" event that ultimately led to the evolution and emergence of the pandemic strain of HIV (HIV-1 group M) in humans (Sauter and Kirchhoff, 2019; Sharp and Hahn, 2011). Like arteriviruses,

Please cite this article in press as: Warren et al., Primate hemorrhagic fever-causing arteriviruses are poised for spillover to humans, Cell (2022), https://doi.org/10.1016/j.cell.2022.09.022

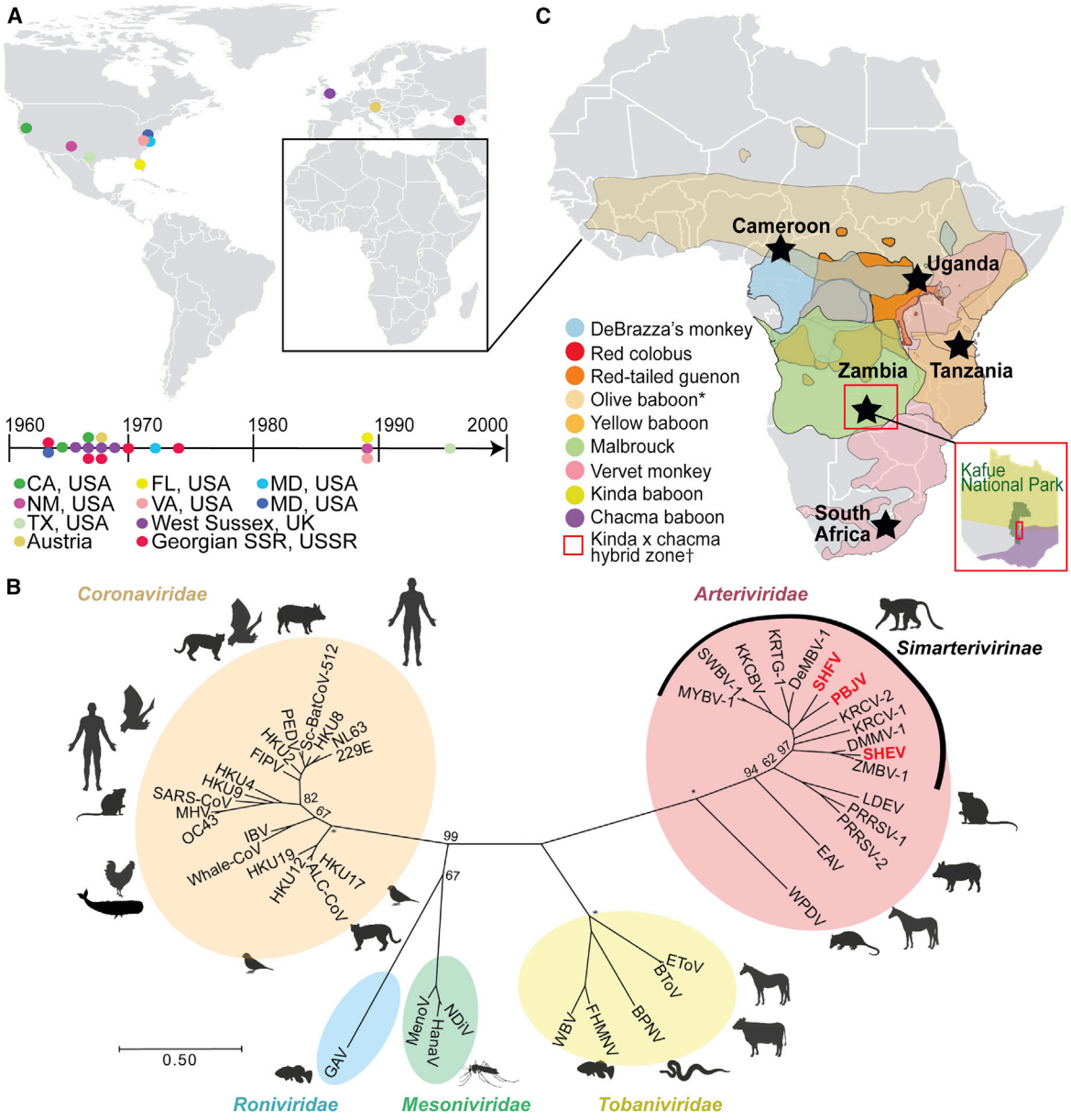

Figure 1. Historical outbreaks and natural reservoirs for simian arteriviruses

(A) Documented simian arterivirus disease outbreaks in primate facilities. Locations of affected facilities are shown by colored circles on the map and timeline. Several facilities experienced multiple outbreaks.

(B) Phylogeny of representative viruses within the order *Nidovirales*, including all published simian arteriviruses, based on an alignment of concatenated RNA-directed RNA polymerase (RdRp) and helicase genes. Arteriviruses known to have caused outbreaks in primate facilities are written in red. The tree is drawn to scale, with branch lengths measured in the number of substitutions per site and bootstrap values shown for major nodes. Asterisks indicate nodes with 100% support.

(C) Geographical ranges of species of primates known to be infected with simian arteriviruses. Sampling sites are indicated by black stars. *Only detected in captivity; †Kafue kinda chacma baboon virus (KKCBV) was discovered in kinda × chacma hybrid baboons, within Kafue National Park, as shown as an inset in red (Chiou et al., 2021).

SIV can cause spillover infection of captive macaques (Daniel et al., 1985; Mansfield et al., 1995). In addition, simian arteriviruses and SIVs are both endemic in African primates (Bailey et al., 2016; Heuverswyn and Peeters, 2007; Lauck et al., 2013; Sharp et al., 2001), cause long-lasting subclinical infections in their hosts (Bailey et al., 2014a, 2014b; Vatter et al., 2015; Wei et al., 1995), have high mutation rates that produce diverse viral swarms (Bailey et al., 2014b; Coffin, 1995; Kuhn et al., 2016), and primarily induce fatal disease after host switching (Bailey et al., 2015; Sharp and Hahn, 2011). Thus, it is important to determine

Please cite this article in press as: Warren et al., Primate hemorrhagic fever-causing arteriviruses are poised for spillover to humans, Cell (2022), https://doi.org/10.1016/j.cell.2022.09.022

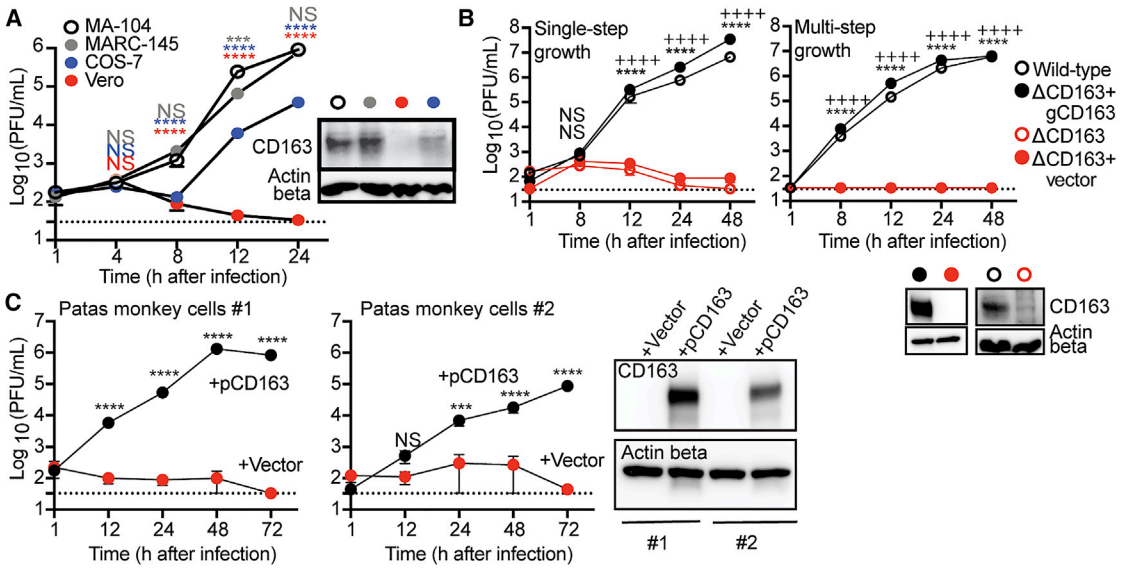

Figure 2. CD163 is necessary and sufficient as the receptor for SHFV infection

(A) SHFV (at a MOI of 3) was incubated with cells from four different grivet cell lines (MA-104, MARC-145, COS-7, and Vero). Infectious virion production over a time course was quantified from cell supernatants by plaque assay (PFU/mL) on permissive MA-104 cells.

(B) Single-step (MOI = 3) and multi-step (MOI = 0.03) growth curves of SHFV on wild-type MA-104 cells and its derivatives: ΔCD163, ΔCD163 complemented with empty vector (ΔCD163 + vector), and ΔCD163 with grivet CD163 (ΔCD163 + gCD163).

(C) Untransformed primary skin fibroblasts derived from a 6-month-old (#1) and a 20-year-old patas monkey (#2) were complemented with empty vector or patas monkey CD163 (pCD163) and exposed to SHFV as described in (A).

(A–C) Lysates from cells were probed for CD163 expression using western blotting. Actin beta served as a loading control. Data show the mean +/− SEM from three independent experiments, with one replicate per experiment. Dotted lines represent the limit of detection for the assay. All plots include error bars; no error bars are shown when the SEM was smaller than the size of the symbols.

Statistical tests used: (A) Two-way ANOVA with Dunnett's post-test when compared to MA-104 cells (***$p < 0.001$, ****$p < 0.0001$; NS, not significant). (B) Two-way ANOVA with Sidak's post-test for wild-type compared to ΔCD163 (****$p < 0.0001$), or for ΔCD163 + vector compared to ΔCD163 + gCD163 (++++$p < 0.0001$), and (C) for + pCD163 compared to + vector cells (***$p < 0.001$, ****$p < 0.0001$).

SHFV, simian hemorrhagic fever virus.

See also Figure S1, S2 and S3.

whether simian arteriviruses have the potential to infect humans (Bailey et al., 2015; Graham and Sullivan, 2018; Warren and Sawyer, 2019). Akin to the example of HIV-1, there is no expectation of resistance in the human population because there are no related human arteriviruses that would give humans cross-protective immunity.

RESULTS

CD163 is necessary and sufficient as the receptor for SHFV infection

Most simian arteriviruses remain uncultured. The few cultured viruses are extremely finicky, replicating in only a handful of nonhuman primate cell lines (Cai et al., 2021; London, 1977; Tauraso et al., 1968; Yú et al., 2016). The best-known simian arterivirus, simian hemorrhagic fever virus (SHFV), was first cultured during a simian hemorrhagic fever outbreak among captive rhesus monkeys (*Macaca mulatta*) at the National Institutes of Health (NIH) Primate Quarantine Unit in Bethesda, Maryland, USA (Palmer et al., 1968; Shelokov et al., 1968; Tauraso et al., 1968). SHFV presumptively entered the macaque population via incidental exposure to fluids from infected African patas monkeys (*Erythrocebus patas*) cohoused at this facility (Dalgard et al., 1992; Gravell et al., 1986; Lauck et al., 2015; London, 1977). *In vitro*, SHFV can only be propagated to high titers on the grivet (*Chlorocebus aethiops*) embryonic kidney MA-104 cell line and its clonal derivatives, such as MARC-145 cells, and a few other cell types (Tauraso et al., 1968; Yú et al., 2016). Grivet cell lines that are routinely used for producing diverse viruses due to their inability to synthesize interferon (Vero cells and subclones) (Desmyter et al., 1968) are not permissive.

Virus entry into mammalian cells is mediated by cellular receptors. For SHFV, we previously found that pre-treating cells with an anti-CD163 antibody impeded infection (Caì et al., 2015; Cai et al., 2021). Based on this clue, we hypothesized that CD163 might be the cellular receptor. Indeed, we found that the relative abundance of CD163 in different grivet cell lines correlates with their relative abilities to produce infectious SHFV (high = MA-104, MARC-145; low = COS-7; none = Vero), potentially corroborating the importance of CD163 expression for SHFV infection (Figure 2A). We next generated CD163 knockout (ΔCD163) single-cell clones of grivet MA-104 cells and confirmed gene deletion (Figure S1). We observed markedly reduced virus production in ΔCD163 cells under single-step and multi-step growth conditions (Figure 2B, open red circles). Stable re-complementation of these cells with grivet CD163 (gCD163) by retroviral

transduction recovered expression and virus production in these cells (Figure 2B, closed black circles). Expression of grivet CD163 in Vero cells also resulted in significant virus production and observable cytopathic effects (Figure S2). Primary skin fibroblasts derived from two different patas monkeys, the presumed natural host of SHFV (Dalgard et al., 1992; Gravell et al., 1986; Lauck et al., 2015; London, 1977), lacked detectable CD163 protein and also did not support virus production. However, stable complementation with patas monkey CD163 (pCD163) rendered cells permissive to infection by SHFV (Figure 2C). Finally, we confirmed that CD163 acts at the step of virus entry into the cell by transfecting ΔCD163 cells with cDNA-launch SHFV rescue plasmids (Cai et al., 2021), effectively bypassing the requirement of CD163 for cellular entry. Transfected ΔCD163 cells produced infectious SHFV but to lower titers, presumably because newly produced virions were incapable of spreading and infecting new cells that lacked CD163 (Figure S3). Therefore, CD163 is necessary and sufficient for infection by SHFV, a finding that should enhance our ability to isolate and study other novel simian arteriviruses that have been historically difficult to propagate *in vitro*.

CD163 is an intracellular receptor

Several hemorrhagic fever-causing viruses that infect humans, such as Lassa virus, Lujo virus, and Ebola virus, use a unique mode of cell entry that involves intracellular receptors (Carette et al., 2011; Jae and Brummelkamp, 2015; Jae et al., 2014; Raaben et al., 2017). After these viruses enter cells, they interact with a receptor embedded in the membranes of late endosomes/lysosomes. Successful engagement allows viruses to fuse with the endolysosomal membrane and enter the cytoplasm; otherwise the virus gets trapped and degraded. Likewise, we noticed that CD163 was undetectable on the surface of permissive primate cells but could be detected via intracellular staining, and that SHFV particles enter cells (non-productively) even in the absence of CD163 (Figure S4). Thus, we hypothesized that CD163 may act as an intracellular receptor for SHFV. To test this hypothesis, we performed single-molecule RNA fluorescence *in situ* hybridization (smFISH) (Femino et al., 1998) to detect viral RNA in cells. To perform smFISH, we tiled 48 DNA oligos antisense to the SHFV genome and then conjugated to each a fluorophore. Once hybridized to the viral RNA, the additive signal of these fluorescently labeled probes enabled the visualization of single SHFV genomes, either by flow cytometry (Figures S3 and S4) or by microscopy. Using confocal microscopy, we observed smFISH puncta (viral RNA) inside both wild-type and ΔCD163 cells 1 h after exposure to virus (Figures 3A and 3B). The signal was transient in ΔCD163 cells and was absent by 4 h post-exposure (Figure 3B), consistent with flow cytometric analysis of similarly exposed cells (Figure S4). By contrast, in wild-type cells, viral RNA persisted and began forming discrete cellular domains by 6 h post-exposure, likely identifying major sites of viral RNA replication (Figure 3A). SHFV particles can therefore enter cells in the absence of CD163, but viral genomes likely become trapped in intracellular vesicles and become degraded.

We next confirmed this finding in primary cells. We isolated monocytes from rhesus monkey whole blood and differentiated them into macrophages using macrophage colony-stimulating factor (M-CSF). Following a short exposure of primary rhesus monkey macrophages to SHFV, viral RNA co-localized with CD163 (Figure 3C). We calculated the association of each fluorescent channel and smFISH puncta (viral RNA) using Pearson's correlation coefficient, a metric of co-localization (Dunn et al., 2011). We found a statistically significant correlation of viral RNA with CD163, but not with Hoechst (DNA, nucleus) or occludin (cell surface protein) staining (Figure 3D). Further, orthogonal views of the z stack images showed smFISH puncta (viral RNA) and CD163 co-localizing within the upper and lower boundaries of the cell, and not at the cell surface, which confirmed the intracellular nature of this interaction (Figure 3E). These findings identify an unusual phenotypic similarity with other zoonotic hemorrhagic fever-causing viruses, i.e., the use of an intracellular receptor.

CD163 is a dynamic barrier to host-switching of SHFV, but the human ortholog is fully functional for SHFV entry

African primates are the long-term reservoir hosts for simian arteriviruses (Bailey et al., 2016; Kuhn et al., 2016). Over evolutionary time, hosts and viruses compete in genetic "arms races," during which each entity experiences natural selection in favor of genetic variants that give them the upper hand (Meyerson and Sawyer, 2011). In the case of receptors, primates are subject to natural selection in favor of mutations that impede virus entry, whereas viruses counter-evolve to regain optimal receptor usage. Indeed, signatures of accelerated evolution can be detected in many virus-receptor pairs (Kaelber et al., 2012; Meyerson et al., 2015; Ng et al., 2015; Warren and Sawyer, 2019; Warren et al., 2019a, 2019b; Demogines et al., 2012, 2013). We found that CD163 has evolved under strong positive natural selection in primates (Figure S5). Nine residue positions in CD163 bear this signature of rapid amino acid replacement over time. CD163 has nine "scavenger receptor cysteine-rich" (SRCR) domains, a transmembrane region, and a cytoplasmic tail (Law et al., 1993). SRCR domains 5 through 9 contain regions important to arterivirus infection (Gorp et al., 2010). Seven of the nine residues under selection map these domains (Figure 4A).

If primates are involved in a genetic arms race with arteriviruses, it is expected that primates of distinct species would encode receptors with radically different tolerances to any specific arterivirus. This is because each species takes a unique evolutionary trajectory in these battles (Meyerson and Sawyer, 2011). We evaluated this expectation by cloning CD163 orthologs from 15 different primate species and stably integrating them into ΔCD163 cells. These cells were then exposed to SHFV to see if they became infected (Figure 4B). As expected, SHFV entered most efficiently by engaging the CD163 ortholog of its presumed natural host, the patas monkey (Figure 4, black bar in graph). Similarly, based on known outbreaks among captive macaques, rhesus monkey CD163 also efficiently facilitated virus entry. However, there were large differences, spanning almost three orders of magnitude, in how well this virus used the CD163 orthologs of other species. The species-specific sequence differences that emerge in virus-receptor arms races have a beneficial side effect to the hosts; they serve as a genetic barrier to virus host switching (Imai and Kawaoka, 2012; Kailasan

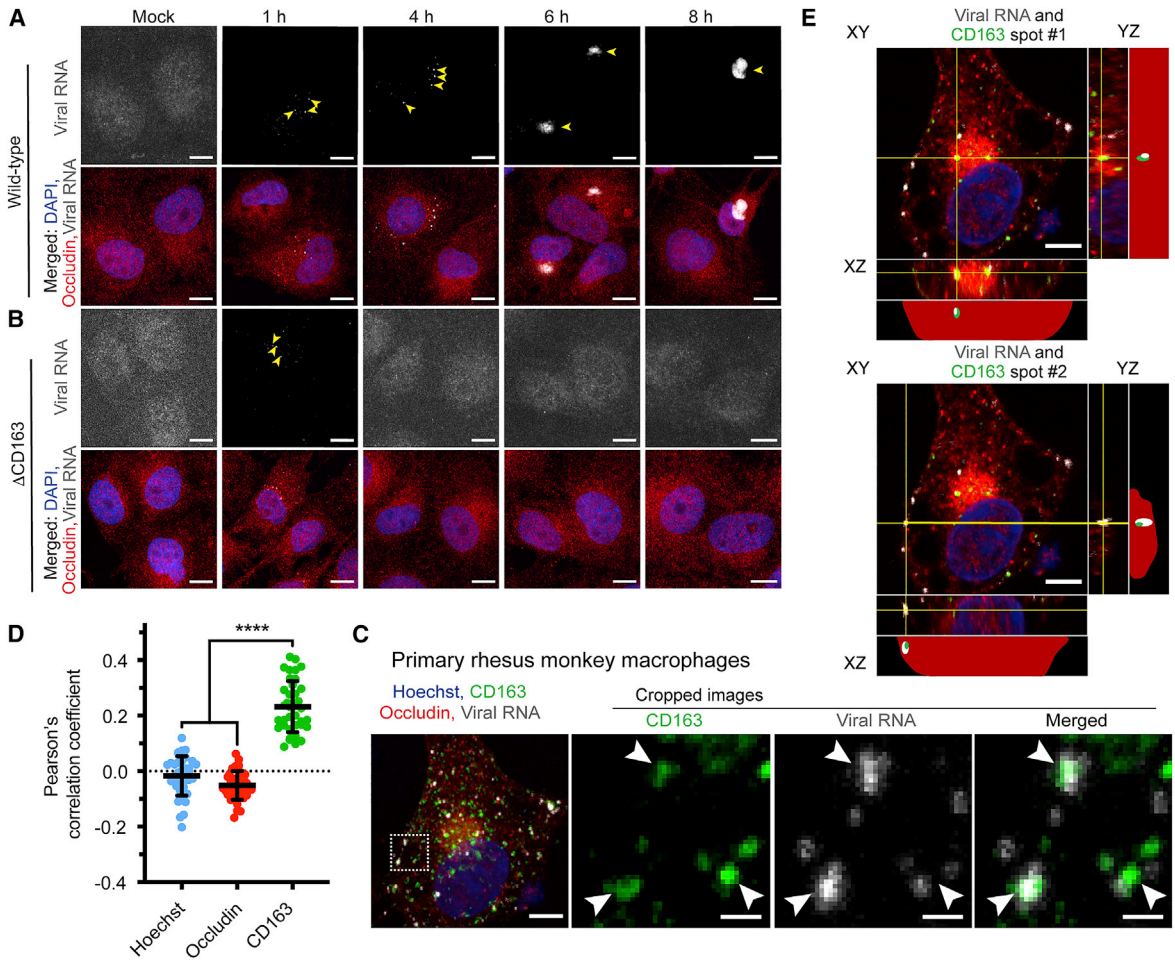

Figure 3. CD163 is an intracellular receptor

(A and B) (A) Wild-type MA-104 or (B) ΔCD163 cells were cultured on glass coverslips and mock-exposed or exposed to simian hemorrhagic fever virus (SHFV) at a MOI of 10 for 1, 4, 6, or 8 h prior to fixation. Cell membranes were immunolabeled (anti-occludin antibody; red) and cells were probed for DNA (4′,6-diamidino-2-phenylindole [DAPI]; blue) and viral RNA (detected by single-molecule RNA fluorescence *in situ* hybridization [smFISH]; gray). Arrows indicate regions of viral RNA signal. Scale bar = 10 μm.

(C) Primary rhesus monkey monocytes were isolated from whole blood and differentiated into macrophages using macrophage colony-stimulating factor (M-CSF). Exposure to SHFV was performed as described above but for 45 min, representing the earliest timepoint that intracellular viral RNA could reliably be detected inside cells. In addition to Hoechst (DNA, nucleus) and occludin staining, cells were immunolabeled to detect CD163 (green). Scale bars = 5 μm (cells) and 1μm (cropped images).

(D) Pearson's correlation analysis of the laser scanning confocal microscopy (LSCM) images generated in the experiment in (C). A Pearson's correlation coefficient (PCC) was calculated between viral RNA signal and either Hoechst (blue), occludin (red), or CD163 (green) signal. Average and standard deviations of each correlation are indicated; each data point represents a single cell. One-way ANOVA with Tukey's post test compared to CD163 signal (**** $p < 0.0001$). The dotted line represents a PCC value of 0.

(E) Single z-planes are shown for two representative images in which viral RNA (gray) and CD163 (green) co-localized and were analyzed in three-dimensional space. The YZ and XZ images are shown for the regions of XY, denoted by the yellow lines and spanning from the top of the imaged cell to the bottom. Actual and simplified illustrations of each orthogonal view are shown, illustrating the relative positions of the viral RNA (gray), CD163 (green), nucleus (blue), and cellular boundaries (red dots). In the simplified view, the red profile is the outline of the cell compiled from z stack images. Scale bar = 5 μm.

(A–C) Cells were imaged by LSCM. A representative maximum intensity projection from each condition is shown. Arrows indicate regions of viral RNA signal. See also Figures S3 and S4.

et al., 2015; Parrish et al., 2008; Warren and Sawyer, 2019). For instance, monkeys of some species are predicted to be resistant to SHFV, based on our finding that the virus does not enter cells efficiently through CD163 of these species (Figure 4B).

Consistent with recent findings that SHFV can replicate in primary cells of the common chimpanzee (*Pan troglodytes*) and western gorilla (*Gorilla gorilla*) (Cai et al., 2021), we found that SHFV is fully compatible with all tested ape CD163 orthologs. Remarkably, this includes the human CD163 ortholog, which supported robust SHFV replication (Figure 4B). These findings are important because they confirm that SHFV has overcome the first hurdle of successful spillover to humans: SHFV virions

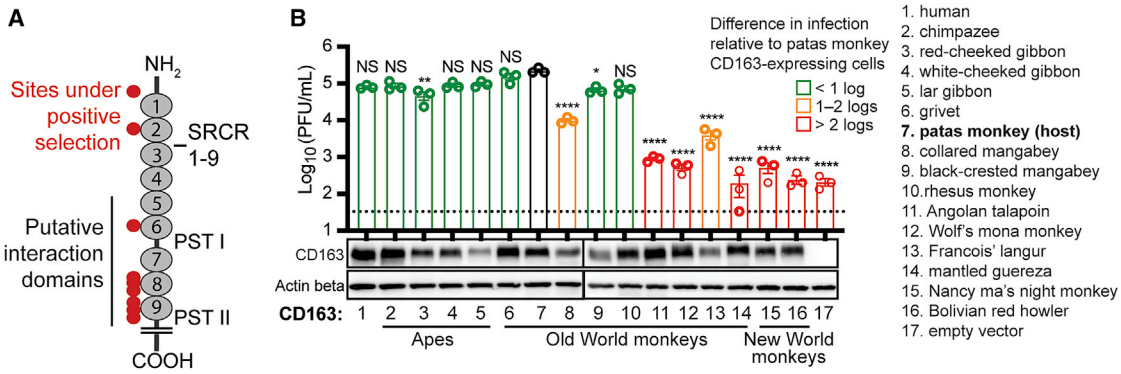

Figure 4. CD163 is a dynamic barrier to host-switching of SHFV, but the human ortholog is fully functional for virus entry

(A) Illustration of the CD163 receptor, showing the extracellular scavenger receptor cysteine-rich (SRCR) domains 1–9, proline domains rich with serine threonine (PST) I and II, and the short cytoplasmic tail. Residues evolving under positive selection are shown with red circles, and the putative arterivirus interaction domain is denoted with a black line. The N terminus (amine terminus; NH_2) and C terminus (carboxyl terminus; COOH) denote the beginning and end of the protein polypeptide chain, respectively.

(B) MA-104 ΔCD163 cells stably expressing the indicated primate CD163 ortholog (x axis) were exposed to SHFV at a MOI of 3. Viral titers in cell supernatants 12 h post-exposure were assessed by plaque assay. Bars are color-coded by log-fold differences in SHFV titers compared to cells expressing the receptor of the presumed natural host (patas monkey; #7).

The data show the mean +/− SEM from three independent experiments, with one replicate per experiment. One-way ANOVA with Dunnett's post-test compared to control cells (*$p < 0.05$, **$p < 0.01$, ****$p < 0.0001$; NS, not significant). The dotted line represents the limit of detection for the assay. CD163 receptor expression was confirmed by western blotting, and actin beta served as a protein loading control.

SHFV, simian hemorrhagic fever virus.

See also Figure S5 and Table S1.

are fully capable of entering cells expressing the human version of their receptor. If CD163 is involved in an evolutionary arms race with simian arteriviruses, then the surface glycoproteins of these viruses are counter-evolving as well—being constantly selected for variants with new receptor binding specificities that could enable them to use receptor orthologs encoded by animals typically resistant to infection.

Human blood monocyte-derived macrophages do not support SHFV infection

Beyond the entry receptor, viruses depend on many host proteins inside of cells to support their replication cycles (Han et al., 2018; Li et al., 2020; Ma et al., 2017; Marceau et al., 2016; Park et al., 2016; Savidis et al., 2016). Although little is known about the life cycle of simian arteriviruses, for other viruses critical human cofactors include proteases, trafficking proteins, etc. For simian arteriviruses to be a threat to humans, they need to be able to use the human orthologs of all the proteins that they require to replicate, and to bypass the interferon response that will be triggered in human cells. CD163 is expressed specifically in myeloid cells, like monocytes and macrophages (Buechler et al., 2000; Fabriek et al., 2005; Maniecki et al., 2006). To test for SHFV replication in primary human cells, monocytes derived from peripheral blood mononuclear cells (PBMCs) from three human donors were differentiated into M0, M1, or M2 macrophages (Figure 5A). We found all of these cell types refractory to SHFV, but susceptible to Ebola virus, which is known to infect macrophages (Figures 5B, 5C and S6). However, little is known about the precise myeloid-derived cell subtypes that SHFV favors (Vatter and Brinton, 2014). Porcine reproductive and respiratory syndrome virus 1 (PRRSV-1, a suid arterivirus) primarily infects subpopulations of tissue-resident macrophages (Duan et al., 1997a; Teifke et al., 2001) and less efficiently infects circulating (blood) monocytes and monocyte-derived cells (Duan et al., 1997b). Similarly, lactate dehydrogenase-elevating virus 1 (LDV-1, a murine arterivirus) has an extremely narrow specificity for a subpopulation of tissue-resident macrophages and is poorly cultivated in macrophages *ex vivo* (Onyekaba et al., 1989; Stueckemann et al., 1982). Further studies on the exact cells that replicate simian arteriviruses *in vivo* are needed, although studies of tissue-embedded immune cell subsets are notoriously difficult (Lee et al., 2018). Based on uncertainties of SHFV tropism in primary cells, we broadened our approach.

SHFV is fully competent for replication in human cells

We next added SHFV to several human monocytic cell lines representing the cellular lineage prior to differentiation into macrophages. We included one monocytic cell line that is naturally CD163-positive (SU-DHL-1) and, as controls, two that are CD163-negative (THP-1 and U937) (Buechler et al., 2000). Remarkably, SHFV produced infectious virus in human SU-DHL-1 cells (Figure 6A). SHFV replication in human cells demonstrates that the compatibility of SHFV with humans extends well beyond the viral receptor and includes the human orthologs of *all* cellular proteins required for viral replication.

To further verify this highly unexpected result, we aimed to demonstrate replication of SHFV in a second human cell line. Previously it was shown that no adherent human cell line in a large human cell panel (the NCI-60 cancer panel) supported SHFV infection (Cai et al., 2021). However, CD163 expression is highly tissue-restricted to myeloid cells, and myeloid cells are not included in that panel. Indeed, western blotting revealed

Please cite this article in press as: Warren et al., Primate hemorrhagic fever-causing arteriviruses are poised for spillover to humans, Cell (2022), https://doi.org/10.1016/j.cell.2022.09.022

CellPress

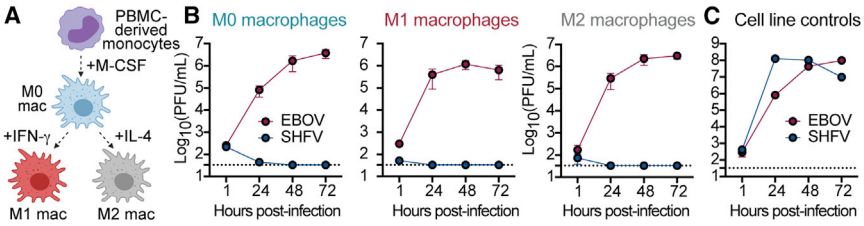

Figure 5. Human blood monocyte-derived macrophages do not support SHFV infection

(A) Monocytes were isolated from human peripheral blood mononuclear cells (PBMCs; n = 3 donors) and differentiated into M0 macrophages. M0 macrophages were further polarized into M1 or M2 subsets using IFN-γ or IL-4, respectively.

(B) Monocyte-derived macrophages were exposed to SHFV or Ebola virus (MOI = 3), and viral titers were enumerated by plaque assay over time. Exposures were performed in technical triplicates, and the mean viral titers from three donors were plotted. Error bars represent SEM. The dotted line represents the limit of detection for the assay.

(C) In parallel, virus stocks were verified as infectious by exposing them to positive control cell lines (MA-104 for SHFV, Vero E6 for Ebola virus). Data are the mean +/− the SD from technical triplicates. The dotted line represents the limit of detection for the assay.

SHFV, simian hemorrhagic fever virus; EBOV, Ebola virus.

See also Figure S6.

that none of the human NCI-60 cell lines expressed CD163 (Figure S7). Consequently, we sought to test whether SHFV could replicate in any of these NCI-60 human cell lines if human CD163 was provided. From four randomly chosen cell lines tested, we found a human kidney epithelial cell line (ACHN) that supported replication of SHFV expressing enhanced green fluorescent protein (SHFV-eGFP) after it was stably transduced with human CD163 (hCD163; Figure 6B). In fact, wild-type SHFV exhibited replication kinetics and viral titers on human CD163-expressing ACHN cells that were the same as those on the most permissive known primate cell line (MA-104; Figure 6C). The virus replicated to high titers on these human cells, producing over 10^7 infectious virions per mL. ACHN cells are documented to be interferon-competent (Shang et al., 2007), leaving us to assume that the virus may escape the human interferon response. Thus, SHFV is able to replicate in human cells, can use the human orthologs of all necessary cofactors, and may bypass interferon mediated pathways of innate immunity. This conclusion is further supported by the fact that SHFV was recently shown to replicate in primary cells of the western gorilla and common chimpanzee (Cai et al., 2021), two apes closely related to humans.

DISCUSSION

We identified CD163 as the intracellular receptor for a primate arterivirus, SHFV. The expression of CD163 is restricted to myeloid cells such as monocytes and macrophages, where it plays an important role in human health (Greaves and Gordon, 2005). When hemoglobin is released into plasma during red blood cell destruction, it is important that it is quickly removed due to the toxicity of its oxidative heme group. Tissue-embedded macrophages take care of this important process, primarily through their CD163 receptor (Kristiansen et al., 2001). Other mammalian arteriviruses have also been associated with CD163 and with tissue-resident monocytes and macrophages (Calvert et al., 2007; Gorp et al., 2010; Huang et al., 2020; Su et al., 2021; Xu et al., 2020; Yu et al., 2020). CD163 is mostly localized intracellularly (Gorp et al., 2009; Nielsen et al., 2006), a common feature shared with many endocytic receptors that traffic between the cell surface and endosomes.

Intracellular processing of the SHFV glycoprotein(s) may be required before CD163 receptor binding can occur. Neutralization experiments utilizing purified soluble grivet CD163 did not prevent SHFV infection (data not shown). This lack of neutralization suggests that arteriviruses, as they circulate in the bloodstream, cannot bind CD163. Instead, we speculate that the unmasking of CD163 binding sites occurs within intracellular compartments. This may function as a mechanism to evade the humoral immune response, as has also been speculated for Ebola virus (Miller et al., 2012), and would be consistent with the observation of persistent arterivirus infections in monkeys (Bailey et al., 2014a, 2014b). This finding has important consequences that need to be prospectively considered in risk scenarios: severe acute respiratory syndrome coronavirus 2 (SARS-CoV-2), which like SHFV is also a nidovirus, in contrast uses a receptor on the cellular surface (ACE2) for cell entry. To do so, SARS-CoV-2 needs to expose its receptor-binding domain prior to adsorbing to cells, thereby leaving it exposed to attack by neutralizing antibodies—the basis for current vaccine approaches. Viruses that use intracellular receptors expose their receptor-binding domains only once inside a cellular compartment. Thus, medical countermeasure development against such viruses is challenging, i.e., strategies that have been successful against SARS-CoV-2 may fail against arteriviruses.

Arteriviruses have been considered relatively obscure since their discovery. However, it should be noted that SIV, and in particular the chimpanzee variant most closely related to the pandemic strain of HIV, was also considered an ''obscure'' virus prior to its discovery in the early years of the HIV/AIDS pandemic (Keele et al., 2006; Sharp and Hahn, 2011). Given the propensity for RNA viruses such as SHFV and SIV to evolve and emerge, ignoring the threat that arteriviruses pose could be unwise.

Our results raise concerns for global health and pandemic prevention. Not only is the human CD163 ortholog compatible with SHFV entry into human cells, but *all* other cellular proteins required for SHFV replication are functional in human cells, as evidenced by SHFV titers of up to 10^7 infectious virions per mL (Figure 6C). Further, we have tested only one of the numerous simian arteriviruses that have been discovered in monkeys (Bailey et al., 2014a, 2016; Lauck et al., 2011, 2013, 2015). They all share the same genetic organization and considerable sequence homology, suggesting that all of them use a similar entry mechanism and that many of them could potentially use human CD163. Further, it appears that interferon-mediated

Please cite this article in press as: Warren et al., Primate hemorrhagic fever-causing arteriviruses are poised for spillover to humans, Cell (2022), https://doi.org/10.1016/j.cell.2022.09.022

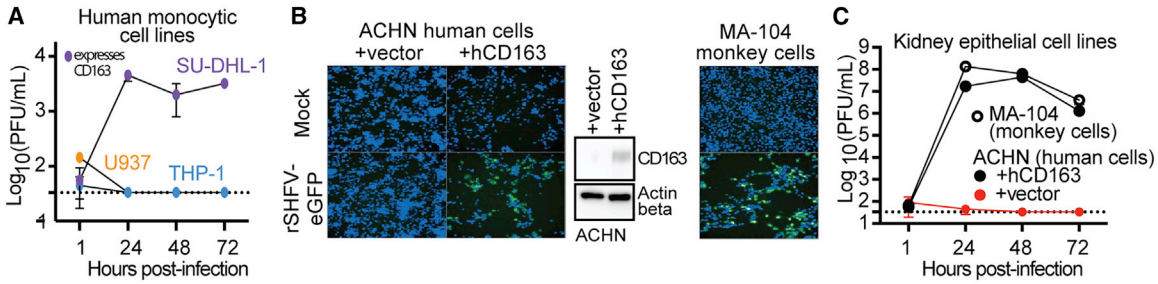

Figure 6. SHFV is fully competent for replication in human cells

(A) Three human monocytic cell lines were exposed to SHFV at a MOI of 0.3. Infectious virus production over a time course was quantified in cell supernatant by plaque assay (PFU/mL) on SHFV-permissive MA-104 cells.

(B) A human cell line was transduced with human CD163 (hCD163) or an empty retroviral vector, and antibiotics were used to select for stable integration. Cells were exposed to recombinant SHFV expressing enhanced green fluorescent protein (rSHFV-eGFP), MOI = 1. Shown are high-content images of mock-exposed or virus-exposed cells counterstained with Hoechst (blue) at 72 h post-exposure. Green fluorescence is indicative of productive viral infection. MA-104 monkey cells served as a positive control.

(C) Wild-type MA-104, along with ACHN kidney cells, stably transduced with human CD163 (hCD163) or empty vector, were exposed to wild-type SHFV (MOI = 0.3).

(A) and (C) Data shown are representative of two independent experiments, each with three technical replicates. Error bars represent the mean +/− SD. The dotted line represents the limit of detection for the assay.

See also Figure S7.

pathways of innate immunity may be ineffective at blocking these viruses, which is concerning given that humans are predicted to be antibody-naive to arteriviruses. Animal studies are not needed before concern for humans is raised, because at least three different simian arteriviruses have already been shown (on numerous occasions) to cause fatal infection in some nonhuman primates.

It is possible that people in Africa are already subclinically infected with arteriviruses. Similar to HIV-1 infections that spread undetected for decades prior to virus discovery in the 1980s (Korber et al., 2000; Worobey et al., 2008), human arterivirus infections may already cause unmeasured disease. HIV-1-induced AIDS kills by secondary infections and hence was etiologically difficult to pinpoint. Simian arterivirus infection may result in a similar scenario, in subclinical infections, or in acute epidemics of hemorrhagic fever. Development of serology tests and other measures for human surveillance will be required to understand and detect human exposure to these viruses. These tools are needed in African regions where endemically infected nonhuman primates live.

Limitations of the study

Despite its breadth, this study has several limitations. SHFV is just one simian arterivirus. Virus stocks do not exist for other arteriviruses that have caused epizootics in the past (i.e., Pebjah virus [PBJV] and simian hemorrhagic encephalitis virus [SHEV]). This limitation prevented us from performing a more systematic study of simian arterivirus diversity. We speculated, based on previous studies, that patas monkeys are the natural reservoir host for SHFV (Dalgard et al., 1992; Gravell et al., 1986; Lauck et al., 2015; London, 1977). However, additional viral surveillance of patas monkeys in the wild is required to determine whether or not they are a possible source of SHFV spillover to humans. Although SHFV-exposed primary human blood monocyte-derived macrophages were incapable of producing infectious virus, this does not provide direct evidence that SHFV cannot replicate in more specialized macrophage subsets. It is possible that alternative subpopulations of tissue-resident macrophages may support SHFV infection, like alveolar macrophages (the target for PRRSV-1 infection in pigs) or peritoneal macrophages (the target for LDV-1 infection in mice).

STAR★METHODS

Detailed methods are provided in the online version of this paper and include the following:

- KEY RESOURCES TABLE
- RESOURCE AVAILABILITY
  - Lead contact
  - Materials availability
  - Data and code availability
- EXPERIMENTAL MODEL AND SUBJECT DETAILS
  - Cells
  - Viruses
- METHOD DETAILS
  - Viral infection assays
  - Western blotting
  - CRISPR-Cas9 editing of CD163
  - CD163 receptor complementation experiments
  - CD163 detection by flow cytometry
  - Design and labeling of smFISH probes
  - Sequential immunofluorescence and smFISH
  - Microscopy and image processing
  - FISH-flow
  - Phylogenetic analysis
  - Evolutionary analysis of positive selection
  - African nonhuman primate range data
- QUANTIFICATION AND STATISTICAL ANALYSIS

SUPPLEMENTAL INFORMATION

Supplemental information can be found online at https://doi.org/10.1016/j.cell.2022.09.022.

ACKNOWLEDGMENTS

We are grateful to Kay Faaberg (U.S. Department of Agriculture National Animal Disease Center, Ames, IA, USA) for providing MA-104 subclone MARC-145 cells, and to Gary Kobinger (Public Health Agency Canada, Winnipeg, MT, Canada) for providing Ebola virus/H.sapiens-wt/GIN/2014/Makona-C05. We thank Nicholas Meyerson, Adam Bailey, and Teressa Shaw for their insightful advice on this work, Jiro Wada for help with data visualization, and Anya Crane for critically editing the manuscript.

This work was funded in part by grants from the National Institutes of Health (NIH) (DP1-DA-046108 and R01-AI-137011 to S.L.S.; F32-GM-125442 and K99-AI151256-01A1 to C.J.W.; R01AI151636 to D.K.P.). S.L.S. is a Burroughs Wellcome Fund Investigator in the Pathogenesis of Infectious Disease. The imaging work was performed at the BioFrontiers Institute Advanced Light Microscopy Core (RRID: SCR_018302). Laser scanning confocal microscopy was performed on a Nikon A1R microscope supported by NIST-CU Cooperative Agreement award number 70NANB15H226. The flow cytometry work was performed at the BioFrontiers Institute Flow Cytometry Core on the BD Accuri C6 Cytometer, supported by NIH Grant S10ODO21601. This work was also supported in part through the Laulima Government Solutions, LLC, prime contract with the National Institutes of Allergy and Infectious Disease (NIAID) under contract number HHSN272201800013C (S.Y., I-C.H., and G.W.); J.H.K. performed this work as an employee of Tunnell Government Services (TGS), a subcontractor of Laulima Government Solutions, LLC, under contract number HHSN272201800013C. The views and conclusions contained in this document are those of the authors and should not be interpreted as necessarily representing the official policies, either expressed or implied, of the U.S. Department of Health and Human Services or of the institutions and companies affiliated with the authors, nor does mention of trade names, commercial products, or organizations imply endorsement by the U.S. Government. In no event shall any of these entities have any responsibility or liability for any use, misuse, inability to use, or reliance upon the information contained herein.

AUTHOR CONTRIBUTIONS

Conceptualization, C.J.W., G.W., I.-C.H., T.L.G., J.H.K., and S.L.S.; methodology, C.J.W., D.K.P., Q.Y., G.W., I.-C.H., J.H.K., and S.L.S.; investigation, C.J.W., S.Y., D.K.P., A.B.-G., B.L.B., and G.K.W.; writing – original draft, C.J.W. and S.L.S.; writing – review & editing, C.J.W., I.-C.H., T.L.G., J.H.K., and S.L.S.; funding acquisition, C.J.W., J.H.K., and S.L.S.; supervision, G.K.W., J.H.K., and S.L.S.

DECLARATION OF INTERESTS

S.L.S. and Q.Y. are co-founders of, equity holders of, and consultants for Darwin Biosciences. S.L.S is on the scientific advisory board for Darwin Biosciences. S.L.S. serves as a consultant for the MITRE Corporation and is a member of the Planning Committee for Countering Zoonotic Spillover of High Consequence Pathogens, sponsored by the U.S. National Academies of Sciences, Engineering, and Medicine.

Received: February 21, 2022
Revised: June 22, 2022
Accepted: September 12, 2022
Published: September 30, 2022

REFERENCES

Aaron, J.S., Taylor, A.B., and Chew, T.-L. (2018). Image co-localization – co-occurrence versus correlation. J Cell Sci. *131* (3), jcs211847. https://doi.org/10.1242/jcs.211847.

Bailey, A.L., Lauck, M., Sibley, S.D., Pecotte, J., Rice, K., Weny, G., Tumukunde, A., Hyeroba, D., Greene, J., Correll, M., et al. (2014a). Two novel simian arteriviruses in captive and wild baboons (*Papio* spp.). J Virol. *88*, 13231–13239. https://doi.org/10.1128/jvi.02203-14.

Bailey, A.L., Lauck, M., Weiler, A., Sibley, S.D., Dinis, J.M., Bergman, Z., Nelson, C.W., Correll, M., Gleicher, M., Hyeroba, D., et al. (2014b). High genetic diversity and adaptive potential of two simian hemorrhagic fever viruses in a wild primate population. PLoS One *9*, e90714. https://doi.org/10.1371/journal.pone.0090714.

Bailey, A.L., Lauck, M., Sibley, S.D., Friedrich, T.C., Kuhn, J.H., Freimer, N.B., Jasinska, A.J., Phillips-Conroy, J.E., Jolly, C.J., Marx, P.A., Apetrei, C., Rogers, J., Goldberg, T.L., and O'Connor, D.H. (2016). Zoonotic potential of simian arteriviruses. J Virol. *90* (2), 630–635. https://doi.org/10.1128/jvi.01433-15.

Bailey, A.L., Lauck, M., Ghai, R.R., Nelson, C.W., Heimbruch, K., Hughes, A.L., Goldberg, T.L., Kuhn, J.H., Jasinska, A.J., Freimer, N.B., et al. (2016). Arteriviruses, pegiviruses, and lentiviruses are common among wild African monkeys. J Virol. *90* (15), 6724–6737. https://doi.org/10.1128/jvi.00573-16.

Baize, S., Pannetier, D., Oestereich, L., Rieger, T., Koivogui, L., Magassouba, N., Soropogui, B., Sow, M.S., Keïta, S., De Clerck, H., et al. (2014). Emergence of Zaire Ebola virus disease in Guinea. New Engl J Med. *371* (15), 1418–1425. https://doi.org/10.1056/nejmoa1404505.

Buechler, C., Ritter, M., Orsó, E., Langmann, T., Klucken, J., and Schmitz, G. (2000). Regulation of scavenger receptor CD163 expression in human monocytes and macrophages by pro- and antiinflammatory stimuli. J Leukoc Biol. *67* (1), 97–103. https://doi.org/10.1002/jlb.67.1.97.

Caì, Y., Postnikova, E.N., Bernbaum, J.G., Yú, S., Mazur, S., Deiuliis, N.M., Radoshitzky, S.R., Lackemeyer, M.G., McCluskey, A., Robinson, P.J., et al. (2015). Simian hemorrhagic fever virus cell entry is dependent on CD163 and uses a clathrin-mediated endocytosis-like pathway. J Virol. *89* (1), 844–856. https://doi.org/10.1128/jvi.02697-14.

Cai, Y., Yu, S., Fang, Y., Bollinger, L., Li, Y., Lauck, M., Postnikova, E.N., Mazur, S., Johnson, R.F., Finch, C.L., et al. (2021). Development and characterization of a cDNA-launch recombinant simian hemorrhagic fever virus expressing enhanced green fluorescent protein: ORF 2b' Is not required for in vitro virus replication. Viruses *13* (4), 632. https://doi.org/10.3390/v13040632.

Calvert, J.G., Slade, D.E., Shields, S.L., Jolie, R., Mannan, R.M., Ankenbauer, R.G., and Welch, S.K. (2007). CD163 expression confers susceptibility to porcine reproductive and respiratory syndrome viruses. J Virol. *81* (14), 7371–7379. https://doi.org/10.1128/jvi.00513-07.

Carette, J.E., Raaben, M., Wong, A.C., Herbert, A.S., Obernosterer, G., Mulherkar, N., Kuehne, A.I., Kranzusch, P.J., Griffin, A.M., Ruthel, G., et al. (2011). Ebola virus entry requires the cholesterol transporter Niemann–Pick C1. Nature *477* (7364), 340–343. https://doi.org/10.1038/nature10348.

Chiou, K.L., Bergey, C.M., Burrell, A.S., Disotell, T.R., Rogers, J., Jolly, C.J., and Phillips-Conroy, J.E. (2021). Genome-wide ancestry and introgression in a Zambian baboon hybrid zone. Mol Ecol. *30* (8), 1907–1920. https://doi.org/10.1111/mec.15858.

Coffin, J.M. (1995). HIV population dynamics in vivo: implications for genetic variation, pathogenesis, and therapy. Science *267* (5197), 483–489. https://doi.org/10.1126/science.7824947.

Dalgard, D.W., Hardy, R.J., Pearson, S.L., Pucak, G.J., Quander, R.V., Zack, P.M., Peters, C.J., and Jahrling, P.B. (1992). Combined simian hemorrhagic fever and Ebola virus infection in cynomolgus monkeys. Lab Anim Sci. *42* (2), 152–157.

Daniel, M.D., Letvin, N.L., King, N.W., Kannagi, M., Sehgal, P.K., Hunt, R.D., Kanki, P.J., Essex, M., and Desrosiers, R.C. (1985). Isolation of T-cell tropic HTLV-III-like retrovirus from macaques. Science *228* (4704), 1201–1204. https://doi.org/10.1126/science.3159089.

Demogines, A., Farzan, M., and Sawyer, S.L. (2012). Evidence for ACE2-utilizing coronaviruses (CoVs) related to severe acute respiratory syndrome CoV in bats. J Virol. *86* (11), 6350–6353. https://doi.org/10.1128/jvi.00311-12.

Demogines, A., Abraham, J., Choe, H., Farzan, M., and Sawyer, S.L. (2013). Dual host-virus arms races shape an essential housekeeping protein. PLoS Biol. *11* (5), e1001571. https://doi.org/10.1371/journal.pbio.1001571.

Desmyter, J., Melnick, J.L., and Rawls, W.E. (1968). Defectiveness of interferon production and of rubella virus interference in a line of African green monkey kidney cells (Vero). J Virol. *2* (10), 955–961. https://doi.org/10.1128/jvi.2.10.955-961.1968.

Duan, X., Nauwynck, H.J., and Pensaert, M.B. (1997a). Virus quantification and identification of cellular targets in the lungs and lymphoid tissues of pigs at different time intervals after inoculation with porcine reproductive and respiratory syndrome virus (PRRSV). Vet Microbiol. *56* (1-2), 9–19. https://doi.org/10.1016/s0378-1135(96)01347-8.

Duan, X., Nauwynck, H.J., and Pensaert, M.B. (1997b). Effects of origin and state of differentiation and activation of monocytes/macrophages on their susceptibility to porcine reproductive and respiratory syndrome virus (PRRSV). Arch Virol. *142* (12), 2483–2497. https://doi.org/10.1007/s007050050256.

Dunn, K.W., Kamocka, M.M., and McDonald, J.H. (2011). A practical guide to evaluating colocalization in biological microscopy. Am J Physiol Cell Physiol *300* (4), C723–C742. –C742. https://doi.org/10.1152/ajpcell.00462.2010.

Fabriek, B.O., Dijkstra, C.D., and van den Berg, T.K. (2005). The macrophage scavenger receptor CD163. Immunobiology *210* (2–4), 153–160. https://doi.org/10.1016/j.imbio.2005.05.010.

Femino, A.M., Fay, F.S., Fogarty, K., and Singer, R.H. (1998). Visualization of single RNA transcripts in situ. Science *280* (5363), 585–590. https://doi.org/10.1126/science.280.5363.585.

Van Gorp, H., Van Breedam, W., Delputte, P.L., and Nauwynck, H.J. (2009). The porcine reproductive and respiratory syndrome virus requires trafficking through CD163-positive early endosomes, but not late endosomes, for productive infection. Arch Virol. *154* (12), 1939–1943. https://doi.org/10.1007/s00705-009-0527-1.

Van Gorp, H., Van Breedam, W., Van Doorsselaere, J., Delputte, P.L., and Nauwynck, H.J. (2010). Identification of the CD163 protein domains involved in infection of the porcine reproductive and respiratory syndrome virus. J Virol. *84* (6), 3101–3105. https://doi.org/10.1128/jvi.02093-09.

Graham, B.S., and Sullivan, N.J. (2018). Emerging viral diseases from a vaccinology perspective: preparing for the next pandemic. Nat Immunol. *19* (1), 20–28. https://doi.org/10.1038/s41590-017-0007-9.

Gravell, M., London, W.T., Leon, M.E., Palmer, A.E., and Hamilton, R.S. (1986). Differences among isolates of simian hemorrhagic fever (SHF) virus. Proc Soc Exp Biol Med. *181* (1), 112–119. https://doi.org/10.3181/00379727-181-42231.

Greaves, D.R., and Gordon, S. (2005). Thematic review series: the immune system and atherogenesis. Recent insights into the biology of macrophage scavenger receptors. J Lipid Res. *46* (1), 11–20. https://doi.org/10.1194/jlr.r400011-jlr200.

Han, J., Perez, J.T., Chen, C., Li, Y., Benitez, A., Kandasamy, M., Lee, Y., Andrade, J., tenOever, B., and Manicassamy, B. (2018). Genome-wide CRISPR/Cas9 screen identifies host factors essential for influenza virus replication. Cell Rep. *23* (2), 596–607. https://doi.org/10.1016/j.celrep.2018.03.045.

Van Heuverswyn, F., and Peeters, M. (2007). The origins of HIV and implications for the global epidemic. Curr Infect Dis Rep. *9* (4), 338–346. https://doi.org/10.1007/s11908-007-0052-x.

Hill, C.M. (2018). Human–primate conflict. In The International Encyclopedia of Biological Anthropology https://doi.org/10.1002/9781118584538.ieba0258.

Hockings, K.J. (2016). Mitigating human–nonhuman primate conflict. In The International Encyclopedia of Primatology https://doi.org/10.1002/9781119179313.wbprim0053.

Hoenen, T., Groseth, A., Feldmann, F., Marzi, A., Ebihara, H., Kobinger, G., Günther, S., and Feldmann, H. (2014). Complete genome sequences of three Ebola virus isolates from the 2014 outbreak in West Africa. Genome Announc. *2* (6). e01331–14. https://doi.org/10.1128/genomea.01331-14.

Huang, C., Bernard, D., Zhu, J., Dash, R.C., Chu, A., Knupp, A., Hakey, A., Hadden, M.K., Garmendia, A., and Tang, Y. (2020). Small molecules block the interaction between porcine reproductive and respiratory syndrome virus and CD163 receptor and the infection of pig cells. Virol J. *17* (1), 116. https://doi.org/10.1186/s12985-020-01361-7.

Imai, M., and Kawaoka, Y. (2012). The role of receptor binding specificity in interspecies transmission of influenza viruses. Curr Opin Virol. *2* (2), 160–167. https://doi.org/10.1016/j.coviro.2012.03.003.

Jae, L.T., and Brummelkamp, T.R. (2015). Emerging intracellular receptors for hemorrhagic fever viruses. Trends Microbiol. *23* (7), 392–400. https://doi.org/10.1016/j.tim.2015.04.006.

Jae, L.T., Raaben, M., Herbert, A.S., Kuehne, A.I., Wirchnianski, A.S., Soh, T.K., Stubbs, S.H., Janssen, H., Damme, M., Saftig, P., et al. (2014). Lassa virus entry requires a trigger-induced receptor switch. Science *344* (6191), 1506–1510. https://doi.org/10.1126/science.1252480.

Johnson, R.F., Dodd, L.E., Yellayi, S., Gu, W., Cann, J.A., Jett, C., Bernbaum, J.G., Ragland, D.R., St Claire, M., Byrum, R., et al. (2011). Simian hemorrhagic fever virus infection of rhesus macaques as a model of viral hemorrhagic fever: clinical characterization and risk factors for severe disease. Virology *421* (2), 129–140. https://doi.org/10.1016/j.virol.2011.09.016.

Jones, D.T., Taylor, W.R., and Thornton, J.M. (1992). The rapid generation of mutation data matrices from protein sequences. Comput Appl Biosci. *8* (3), 275–282. https://doi.org/10.1093/bioinformatics/8.3.275.

Kaelber, J.T., Demogines, A., Harbison, C.E., Allison, A.B., Goodman, L.B., Ortega, A.N., Sawyer, S.L., and Parrish, C.R. (2012). Evolutionary reconstructions of the transferrin receptor of caniforms supports canine parvovirus being a re-emerged and not a novel pathogen in dogs. PLoS Pathog. *8* (5), e1002666. https://doi.org/10.1371/journal.ppat.1002666.

Kailasan, S., Agbandje-McKenna, M., and Parrish, C.R. (2015). Parvovirus family conundrum: what makes a killer? Ann Rev Virol. *2* (1), 425–450. https://doi.org/10.1146/annurev-virology-100114-055150.

Keele, B.F., Van Heuverswyn, F., Li, Y., Bailes, E., Takehisa, J., Santiago, M.L., Bibollet-Ruche, F., Chen, Y., Wain, L.V., Liegeois, F., et al. (2006). Chimpanzee reservoirs of pandemic and nonpandemic HIV-1. Science *313* (5786), 523–526. https://doi.org/10.1126/science.1126531.

Korber, B., Muldoon, M., Theiler, J., Gao, F., Gupta, R., Lapedes, A., Hahn, B.H., Wolinsky, S., and Bhattacharya, T. (2000). Timing the ancestor of the HIV-1 pandemic strains. Science *288* (5472), 1789–1796. https://doi.org/10.1126/science.288.5472.1789.

Kristiansen, M., Graversen, J.H., Jacobsen, C., Sonne, O., Hoffman, H.-J., Law, S.A., and Moestrup, S.K. (2001). Identification of the haemoglobin scavenger receptor. Nature *409* (6817), 198–201. https://doi.org/10.1038/35051594.

Kuhn, J.H., Lauck, M., Bailey, A.L., Shchetinin, A.M., Vishnevskaya, T.V., Bào, Y., Ng, T.F., LeBreton, M., Schneider, B.S., Gillis, A., et al. (2016). Reorganization and expansion of the nidoviral family *Arteriviridae*. Arch Virol. *161* (3), 755–768. https://doi.org/10.1007/s00705-015-2672-z.

Kumar, S., Stecher, G., and Tamura, K. (2016). MEGA7: molecular evolutionary genetics analysis version 7.0 for bigger datasets. Mol Biol Evol. *33* (7), 1870–1874. https://doi.org/10.1093/molbev/msw054.

Lauck, M., Hyeroba, D., Tumukunde, A., Weny, G., Lank, S.M., Chapman, C.A., O'Connor, D.H., Friedrich, T.C., and Goldberg, T.L. (2011). Novel, divergent simian hemorrhagic fever viruses in a wild Ugandan red colobus monkey discovered using direct pyrosequencing. PLoS One *6* (4), e19056. https://doi.org/10.1371/journal.pone.0019056.

Lauck, M., Sibley, S.D., Hyeroba, D., Tumukunde, A., Weny, G., Chapman, C.A., Ting, N., Switzer, W.M., Kuhn, J.H., Friedrich, T.C., et al. (2013). Exceptional simian hemorrhagic fever virus diversity in a wild African primate community. J Virol. *87* (1), 688–691. https://doi.org/10.1128/jvi.02433-12.

Lauck, M., Palacios, G., Wiley, M.R., Lǐ, Y., Fāng, Y., Lackemeyer, M.G., Caì, Y., Bailey, A.L., Postnikova, E., Radoshitzky, S.R., et al. (2014). Genome sequences of simian hemorrhagic fever virus variant NIH LVR42-0/M6941 isolates (*Arteriviridae*: Arterivirus). Genome Announc. *2* (5), e00978-14. https://doi.org/10.1128/genomea.00978-14.

Lauck, M., Alkhovsky, S.V., Bào, Y., Bailey, A.L., Shevtsova, Z.V., Shchetinin, A.M., Vishnevskaya, T.V., Lackemeyer, M.G., Postnikova, E., Mazur, S., et al. (2015). Historical outbreaks of simian hemorrhagic fever in captive macaques were caused by distinct arteriviruses. J Virol. *89* (15), 8082–8087. https://doi.org/10.1128/jvi.01046-15.

Law, S.K., Micklem, K.J., Shaw, J.M., Zhang, X.P., Dong, Y., Willis, A.C., and Mason, D.Y. (1993). A new macrophage differentiation antigen which is a member of the scavenger receptor superfamily. Eur J Immunol. *23* (9), 2320–2325. https://doi.org/10.1002/eji.1830230940.

Lee, C.Z.W., Kozaki, T., and Ginhoux, F. (2018). Studying tissue macrophages in vitro: are iPSC-derived cells the answer? Nat Rev Immunol. *18* (11), 716–725. https://doi.org/10.1038/s41577-018-0054-y.

Li, B., Clohisey, S.M., Chia, B.S., Wang, B., Cui, A., Eisenhaure, T., Schweitzer, L.D., Hoover, P., Parkinson, N.J., Nachshon, A., et al. (2020). Genome-wide CRISPR screen identifies host dependency factors for influenza A virus infection. Nat Commun. *11* (1), 164. https://doi.org/10.1038/s41467-019-13965-x.

Logue, J., Vargas Licona, W., Cooper, T., Reeder, B., Byrum, R., Qin, J., Deiuliis Murphy, N., Cong, Y., Bonilla, A., Sword, J., et al. (2019). Ebola virus isolation using Huh-7 cells has methodological advantages and similar sensitivity to isolation using other cell types and suckling BALB/c laboratory mice. Viruses *11* (2), 161. https://doi.org/10.3390/v11020161.

London, W.T. (1977). Epizootiology, transmission and approach to prevention of fatal simian haemorrhagic fever in rhesus monkeys. Nature *268* (5618), 344–345. https://doi.org/10.1038/268344a0.

Ma, Y., Walsh, M.J., Bernhardt, K., Ashbaugh, C.W., Trudeau, S.J., Ashbaugh, I.Y., Jiang, S., Jiang, C., Zhao, B., Root, D.E., et al. (2017). CRISPR/Cas9 screens reveal Epstein-Barr virus-transformed B cell host dependency factors. Cell Host Microbe *21* (5), 580–591.e7. https://doi.org/10.1016/j.chom.2017.04.005.

Maniecki, M.B., Møller, H.J., Moestrup, S.K., and Møller, B.K. (2006). CD163 positive subsets of blood dendritic cells: the scavenging macrophage receptors CD163 and CD91 are coexpressed on human dendritic cells and monocytes. Immunobiology *211* (6–8), 407–417. https://doi.org/10.1016/j.imbio.2006.05.019.

Mansfield, K.G., Lerche, N.W., Gardner, M.B., and Lackner, A.A. (1995). Origins of simian immunodeficiency virus infection in macaques at the New England Regional Primate Research Center. J Med Primatol. *24* (3), 116–122. https://doi.org/10.1111/j.1600-0684.1995.tb00156.x.

Marceau, C.D., Puschnik, A.S., Majzoub, K., Ooi, Y.S., Brewer, S.M., Fuchs, G., Swaminathan, K., Mata, M.A., Elias, J.E., Sarnow, P., and Carette, J.E. (2016). Genetic dissection of *Flaviviridae* host factors through genome-scale CRISPR screens. Nature *535* (7610), 159–163. https://doi.org/10.1038/nature18631.

Meyerson, N.R., and Sawyer, S.L. (2011). Two-stepping through time: mammals and viruses. Trends Microbiol. *19* (6), 286–294. https://doi.org/10.1016/j.tim.2011.03.006.

Meyerson, N.R., Sharma, A., Wilkerson, G.K., Overbaugh, J., and Sawyer, S.L. (2015). Identification of owl monkey CD4 receptors broadly compatible with early-stage HIV-1 Isolates. J Virol. *89* (16), 8611–8622. https://doi.org/10.1128/jvi.00890-15.

Miller, E.H., Obernosterer, G., Raaben, M., Herbert, A.S., Deffieu, M.S., Krishnan, A., Ndungo, E., Sandesara, R.G., Carette, J.E., Kuehne, A.I., et al. (2012). Ebola virus entry requires the host-programmed recognition of an intracellular receptor. EMBO J. *31* (8), 1947–1960. https://doi.org/10.1038/emboj.2012.53.

Ng, M., Ndungo, E., Kaczmarek, M.E., Herbert, A.S., Binger, T., Kuehne, A.I., Jangra, R.K., Hawkins, J.A., Gifford, R.J., Biswas, R., et al. (2015). Filovirus receptor NPC1 contributes to species-specific patterns of ebolavirus susceptibility in bats. Elife *4*, e11785. https://doi.org/10.7554/elife.11785.

Nga, P.T., Parquet, M.del.C., Lauber, C., Parida, M., Nabeshima, T., Yu, F., Thuy, N.T., Inoue, S., Ito, T., Okamoto, K., et al. (2011). Discovery of the first insect nidovirus, a missing evolutionary link in the emergence of the largest RNA virus genomes. PLoS Pathog. *7* (9), e1002215. https://doi.org/10.1371/journal.ppat.1002215.

Nielsen, M.J., Madsen, M., Møller, H.J., and Moestrup, S.K. (2006). The macrophage scavenger receptor CD163: endocytic properties of cytoplasmic tail variants. J Leukoc Biol. *79* (4), 837–845. https://doi.org/10.1189/jlb.1005602.

Onyekaba, C.O., Harty, J.T., and Plagemann, P.G. (1989). Extensive cytocidal replication of lactate dehydrogenase-elevating virus in cultured peritoneal macrophages from 1–2-week-old mice. Virus Res. *14* (4), 327–338. https://doi.org/10.1016/0168-1702(89)90025-7.

Paige, S.B., Bleecker, J., Mayer, J., and Goldberg, T. (2017). Spatial overlap between people and non-human primates in a fragmented landscape. EcoHealth *14* (1), 88–99. https://doi.org/10.1007/s10393-016-1194-9.

Paige, S.B., Frost, S.D., Gibson, M.A., Jones, J.H., Shankar, A., Switzer, W.M., Ting, N., and Goldberg, T.L. (2014). Beyond bushmeat: animal contact, injury, and zoonotic disease risk in Western Uganda. Ecohealth *11* (4), 534–543. https://doi.org/10.1007/s10393-014-0942-y.

Palmer, A.E., Shelokov, A., Allen, A.M., and Tauraso, N.M. (1968). Simian hemorrhagic fever. I. Clinical and epizootiologic aspects of an outbreak among quarantined monkeys. Am J Trop Med Hyg. *17* (3), 404–412. https://doi.org/10.4269/ajtmh.1968.17.404.

Park, R.J., Wang, T., Koundakjian, D., Hultquist, J.F., Lamothe-Molina, P., Monel, B., Schumann, K., Yu, H., Krupzcak, K.M., Garcia-Beltran, W., et al. (2016). A genome-wide CRISPR screen identifies a restricted set of HIV host dependency factors. Nat Genet. *49* (2), 193–203. https://doi.org/10.1038/ng.3741.

Parrish, C.R., Holmes, E.C., Morens, D.M., Park, E.C., Burke, D.S., Calisher, C.H., Laughlin, C.A., Saif, L.J., and Daszak, P. (2008). Cross-species virus transmission and the emergence of new epidemic diseases. Microbiol Mol Biol Rev. *72* (3), 457–470. https://doi.org/10.1128/mmbr.00004-08.

Perelman, P., Johnson, W.E., Roos, C., Seuánez, H.N., Horvath, J.E., Moreira, M.A.M., Kessing, B., Pontius, J., Roelke, M., Rumpler, Y., et al. (2011). A molecular phylogeny of living primates. PLoS Genet. *7* (3), e1001342. https://doi.org/10.1371/journal.pgen.1001342.

Perrière, G., and Gouy, M. (1996). WWW-query: An on-line retrieval system for biological sequence banks. Biochimie *78* (5), 364–369. https://doi.org/10.1016/0300-9084(96)84768-7.

Peters, D.K., and Garcea, R.L. (2020). Murine polyomavirus DNA transitions through spatially distinct nuclear replication subdomains during infection. PLoS Pathog. *16* (3), e1008403. https://doi.org/10.1371/journal.ppat.1008403.

Raaben, M., Jae, L.T., Herbert, A.S., Kuehne, A.I., Stubbs, S.H., Chou, Y.Y., Blomen, V.A., Kirchhausen, T., Dye, J.M., Brummelkamp, T.R., and Whelan, S.P. (2017). NRP2 and CD63 are host factors for Lujo virus cell entry. Cell Host Microbe *22* (5), 688–696.e5. https://doi.org/10.1016/j.chom.2017.10.002.

Sauter, D., and Kirchhoff, F. (2019). Key viral adaptations preceding the AIDS pandemic. Cell Host Microbe *25* (1), 27–38. https://doi.org/10.1016/j.chom.2018.12.002.

Savidis, G., McDougall, W.M., Meraner, P., Perreira, J.M., Portmann, J.M., Trincucci, G., John, S.P., Aker, A.M., Renzette, N., Robbins, D.R., et al. (2016). Identification of Zika virus and dengue virus dependency factors using functional genomics. Cell Rep. *16* (1), 232–246. https://doi.org/10.1016/j.celrep.2016.06.028.

Schneider, C.A., Rasband, W.S., and Eliceiri, K.W. (2012). NIH Image to ImageJ: 25 years of image analysis. Nat Methods *9* (7), 671–675. https://doi.org/10.1038/nmeth.2089.

Shang, D., Liu, Y., Ito, N., Kamoto, T., and Ogawa, O. (2007). Defective Jak–Stat activation in renal cell carcinoma is associated with interferon-α resistance. Cancer Sci. *98* (8), 1259–1264. https://doi.org/10.1111/j.1349-7006.2007.00526.x.

Sharp, P.M., and Hahn, B.H. (2011). Origins of HIV and the AIDS pandemic. Cold Spring Harb Perspect Med. *1* (1), a006841. https://doi.org/10.1101/cshperspect.a006841.

Sharp, P.M., Bailes, E., Chaudhuri, R.R., Rodenburg, C.M., Santiago, M.O., and Hahn, B.H. (2001). The origins of acquired immune deficiency syndrome viruses: where and when? Philos Trans R Soc Lond B Biol Sci. *356* (1410), 867–876. https://doi.org/10.1098/rstb.2001.0863.

Allen, A.M., Shelokov, A., Tauraso, N.M., and Palmer, A.E. (1968). Simian hemorrhagic fever: II. Studies in pathology. Am J Trop Med Hyg. *17* (3), 413–421. https://doi.org/10.4269/ajtmh.1968.17.413.

Stecher, G., Tamura, K., and Kumar, S. (2020). Molecular evolutionary genetics analysis (MEGA) for macOS. Mol Biol Evol. *37* (4), 1237–1239. https://doi.org/10.1093/molbev/msz312.

Stueckemann, J.A., Holth, M., Swart, W.J., Kowalchyk, K., Smith, M.S., Wolstenholme, A.J., Cafruny, W.A., and Plagemann, P.G. (1982). Replication of Lactate Dehydrogenase-elevating Virus in Macrophages: 2. Mechanism of Persistent Infection in Mice and Cell Culture. J Gen Virol. *59* (Pt 2), 263–272. https://doi.org/10.1099/0022-1317-59-2-263.

Su, C.M., Rowland, R.R.R., and Yoo, D. (2021). Recent advances in PRRS virus receptors and the targeting of receptor–ligand for control. Vaccines (Basel) *9* (4), 354. https://doi.org/10.3390/vaccines9040354.

Suyama, M., Torrents, D., and Bork, P. (2006). PAL2NAL: robust conversion of protein sequence alignments into the corresponding codon alignments. Nucleic Acids Res. *34*, W609–W612. https://doi.org/10.1093/nar/gkl315.

Tauraso, N.M., Allen, A.M., Palmer, A.E., and Shelokov, A. (1968). Simian hemorrhagic fever. 3. Isolation and characterization of a viral agent. Am J Trop Med Hyg. *17* (3), 422–431. https://doi.org/10.4269/ajtmh.1968.17.422.

Teifke, J.P., Dauber, M., Fichtner, D., Lenk, M., Polster, U., Weiland, E., and Beyer, J. (2001). Detection of European porcine reproductive and respiratory syndrome virus in porcine alveolar macrophages by two-colour immunofluorescence and in-situ hybridization-immunohistochemistry double labelling. J Comp Pathol. *124* (4), 238–245. https://doi.org/10.1053/jcpa.2000.0458.

Vatter, H.A., and Brinton, M.A. (2014). Differential responses of disease-resistant and disease-susceptible primate macrophages and myeloid dendritic cells to simian hemorrhagic fever virus infection. J Virol. *88* (4), 2095–2106. https://doi.org/10.1128/jvi.02633-13.

Vatter, H.A., Donaldson, E.F., Huynh, J., Rawlings, S., Manoharan, M., Legasse, A., Planer, S., Dickerson, M.F., Lewis, A.D., Colgin, L.M., et al. (2015). A simian hemorrhagic fever virus isolate from persistently infected baboons efficiently induces hemorrhagic fever disease in Japanese macaques. Virology *474*, 186–198. https://doi.org/10.1016/j.virol.2014.10.018.

Warren, C.J., and Sawyer, S.L. (2019). How host genetics dictates successful viral zoonosis. PLoS Biol. *17* (4), e3000217. https://doi.org/10.1371/journal.pbio.3000217.

Warren, C.J., Meyerson, N.R., Dirasantha, O., Feldman, E.R., Wilkerson, G.K., and Sawyer, S.L. (2019a). Selective use of primate CD4 receptors by HIV-1. PLoS Biol. *17* (6), e3000304. https://doi.org/10.1371/journal.pbio.3000304.

Warren, C.J., Meyerson, N.R., Stabell, A.C., Fattor, W.T., Wilkerson, G.K., and Sawyer, S.L. (2019b). A glycan shield on chimpanzee CD4 protects against infection by primate lentiviruses (HIV/SIV). Proc Natl Acad Sci U S A *116* (23), 11460–11469. https://doi.org/10.1073/pnas.1813909116.

Wei, X., Ghosh, S.K., Taylor, M.E., Johnson, V.A., Emini, E.A., Deutsch, P., Lifson, J.D., Bonhoeffer, S., Nowak, M.A., Hahn, B.H., et al. (1995). Viral dynamics in human immunodeficiency virus type 1 infection. Nature *373* (6510), 117–122. https://doi.org/10.1038/373117a0.

Worobey, M., Gemmel, M., Teuwen, D.E., Haselkorn, T., Kunstman, K., Bunce, M., Muyembe, J.J., Kabongo, J.M., Kalengayi, R.M., Van Marck, E., et al. (2008). Direct evidence of extensive diversity of HIV-1 in Kinshasa by 1960. Nature *455* (7213), 661–664. https://doi.org/10.1038/nature07390.

Xu, H., Liu, Z., Zheng, S., Han, G., and He, F. (2020). CD163 antibodies inhibit PRRSV infection via receptor blocking and transcription suppression. Vaccines (Basel) *8* (4), 592. https://doi.org/10.3390/vaccines8040592.

Yamashita, M., and Emerman, M. (2004). Capsid Is a dominant determinant of retrovirus infectivity in nondividing cells. J Virol. *78* (11), 5670–5678. https://doi.org/10.1128/jvi.78.11.5670-5678.2004.

Yang, Z. (2007). PAML 4: phylogenetic analysis by maximum likelihood. Mol Biol Evol. *24* (8), 1586–1591. https://doi.org/10.1093/molbev/msm088.

Yu, P., Wei, R., Dong, W., Zhu, Z., Zhang, X., Chen, Y., Liu, X., and Guo, C. (2019). CD163ΔSRCR5 MARC-145 cells resist PRRSV-2 infection via inhibiting virus uncoating, which requires the interaction of CD163 with calpain 1. Front Microbiol. *10*, 3115. https://doi.org/10.3389/fmicb.2019.03115.

Yú, S., Caì, Y., Lyons, C., Johnson, R.F., Postnikova, E., Mazur, S., Johnson, J.C., Radoshitzky, S.R., Bailey, A.L., Lauck, M., et al. (2016). Specific detection of two divergent simian arteriviruses using RNAscope in situ hybridization. PLoS One *11* (3), e0151313. https://doi.org/10.1371/journal.pone.0151313.

Please cite this article in press as: Warren et al., Primate hemorrhagic fever-causing arteriviruses are poised for spillover to humans, Cell (2022), https://doi.org/10.1016/j.cell.2022.09.022

STAR★METHODS

KEY RESOURCES TABLE

REAGENT or RESOURCE	SOURCE	IDENTIFIER
Antibodies		
Goat polyclonal anti-CD163	R&D Systems	Cat#AF1607; RRID:AB_354889
Mouse monoclonal anti-actin beta (clone 8H10D10)	Cell Signaling Technology	Cat#3700S; AB_2242334
Donkey anti-goat IgG (H + L) HRP conjugate	Thermo Fisher Scientific	Cat#A16005; AB_2534679
Anti-mouse IgG (H + L) HRP conjugate	Promega	Cat#W4021; AB_430834
Mouse purified monoclonal anti-CD163 (clone GHI/61)	BioLegend	Cat#333609; AB_2291272
Rabbit polyclonal anti-occludin	Thermo Fisher Scientific	Cat#71-1500; AB_88065
Goat anti-mouse IgG AF488+	Invitrogen	Cat#A32723; AB_2633275
Goat anti-rabbit IgG AF546	Invitrogen	Cat#A-11010; AB_2534077
Bacterial and virus strains		
Simian hemorrhagic fever virus (SHFV) isolate LVR42-0/M6941	American Type Culture Collection (ATCC)	Cat#VR-533
Ebola virus/H.sapiens-wt/GIN/2014/Makona-C05	Gary Kobinger (Public Health Agency Canada)	N/A
Biological samples		
Rhesus monkey peripheral blood mononuclear cells (PBMCs)	G. K. Wilkerson, The University of Texas MD Anderson Cancer Center	N/A
Human PBMCs	Lonza	Cat#4W-270A
Nancy Ma's night monkey (*Aotus nancymaae*) PBMCs	G. K. Wilkerson	N/A
Chemicals, peptides, and recombinant proteins		
Human recombinant macrophage colony-stimulating factor (M-CSF)	R&D Systems	Cat#216-MC-010
Interferon-γ (IFN-γ)	R&D Systems	Cat#285-IF
Interleukin 4 (IL-4)	MilliporeSigma	Cat#H7291
Polybrene hexadimethrine bromide	MilliporeSigma	107,689-10G
5-propargylamino-2′,3′-dideoxyuridine-5′-triphosphate (ddUTP) ATTO 633	Jena Bioscience	Cat#NU-1619-633
Cas9 nuclease, S. pyogenes	New England Biolabs (NEB)	Cat#M0386M
Eagle's minimum essential medium (EMEM)	ATCC	30–2003
10% fetal bovine serum (FBS)	MilliporeSigma	TMS-013-B
1X penicillin-streptomycin solution (Pen Strep)	Avantor	#45000-652
RPMI-1640 medium	ATCC	#30-2001
Dulbecco's modified Eagle's medium (DMEM)	MilliporeSigma	#D6429
L-glutamine	Corning Incorporated	#MT25005CI
Hygromycin	Corning Incorporated	#30-240-CR
PBS (PBS)	Caisson Labs	PBL01-6X500ML
ImmunoCult-SF macrophage medium	STEMCELL Technologies	#10961
1X phenol-free EMEM	VWR	#115-073-101
1.4% Avicel	FMC Corporation	RC-591 NF

(*Continued on next page*)

Please cite this article in press as: Warren et al., Primate hemorrhagic fever-causing arteriviruses are poised for spillover to humans, Cell (2022), https://doi.org/10.1016/j.cell.2022.09.022

Continued

REAGENT or RESOURCE	SOURCE	IDENTIFIER
10% neutral buffered formalin	MilliporeSigma	#HT501128-4L
0.2% crystal violet	MilliporeSigma	#C3866-25G
Lipofectamine 3000 reagent	Thermo Fisher Scientific	#L3000008
Opti-MEM	Thermo Fisher Scientific	#31985-070
Tragacanth	MilliporeSigma	#G1128
Nonidet P-40 buffer (NP-40)	Promega	#V4221
Tris(hydroxymethyl)aminomethane hydrochloride (HCl) pH 7.4	Teknova	#T1075
1% NP-40	G-Biosciences	#DG001
Dithiothreitol (DTT)	IBI Scientific	#IB21040
Benzonase	MilliporeSigma	#E1014
Protease inhibitor mixture	MilliporeSigma	#11873580001
EDTA	Corning Incorporated	#25-052-CI
10% Tris-glycine eXtended (TGX) stain-free acrylamide premixed gel solution	Bio-Rad	#1610182
0.1% tris-buffered saline (TBS)	Research Products International (RPI)	#T60075–4000.0
Polysorbate 20	Amresco	#M147-1L
Nestlé Carnation 5% nonfat dried milk	Vevey	N/A
Enhanced chemiluminescent (ECL) reagent	MilliporeSigma	#GERPN2232
Neon Transfection System Kit	Thermo Fisher Scientific	#MPK10025
T7 endonuclease 1 (E1) assay in the Alt-R Genome Editing Detection Kit	Integrated DNA Technologies (IDT)	#1075931
Phusion high-fidelity polymerase chain reaction (PCR) master mix with buffer	NEB	#M0531L
Clontech pLHCX retroviral expression vector	Takara Bio Inc.	#631511
TransIT 293 transfection reagent	Mirus Bio	#MIR2705
4% PFA	VWR	#100504-858
FACS buffer	MilliporeSigma	#324506-100ML
Terminal deoxynucleotidyl transferase (TdT) buffer	Thermo Fisher Scientific	#EP0161
Sodium acetate (NaOAc)	Amresco	#E498-200ML
100% cold ethanol (EtOH)	Thermo Fisher Scientific	# 04-355-223
Nuclease-free water	IBI Scientific	# IB42201
Poly-L-lysine	MilliporeSigma	#P8920
Paraformaldehyde (PFA)	VWR	#100504-85
0.1% Triton X-100	VWR	#JTX198-5
Wash Buffer A	Biosearch Technologies	#SMF-WA1-60
Hybridization buffer	Biosearch Technologies	#SMF-HB1-10
Hoechst 33,342 dye for DNA and nuclei	Invitrogen	#H3570
Wash Buffer B	Biosearch Technologies	#SMF-WB1-20
Prolong Gold Antifade Mountant with 4′,6-diamidino-2-phenylindole (DAPI)	Thermo Fisher Scientific	#P36941
10% neutral buffered formalin	VWR	#16004-128
Critical commercial assays		
Bicinchoninic acid (BCA) protein assay	Thermo Fisher Scientific	Cat#23227
Alt-R Genome Editing Detection Kit	IDT	Cat#1075931
TOPO TA cloning kit	Thermo Fisher Scientific	Cat#K457501
Cytofix/cytoperm Fixation/Permeabilization solution kit	BD	Cat#554714
Data and code availability		

(*Continued on next page*)

Please cite this article in press as: Warren et al., Primate hemorrhagic fever-causing arteriviruses are poised for spillover to humans, Cell (2022), https://doi.org/10.1016/j.cell.2022.09.022

Continued

REAGENT or RESOURCE	SOURCE	IDENTIFIER
CD163 receptor orthologs cloned from nonhuman primate biomaterial	This study	GenBank: MZ695198 toMZ695214
Pearson correlation coefficient analysis	Peters and Garcea (2020)	https://github.com/DouglasPeters/GarceaMatLabAnalyses/blob/52257dea52d610218b7b9b8b7b43818de67f72de/SIM_ColocalizationandCovarianceAnalysis_08152019_CURRENT.m
Experimental models: Cell lines		
MA-104 Clone 1	ATCC	Cat#CRL-2378.1
MA-104 subclone MARC-145	Kay Faaberg, U.S. Department of Agriculture	N/A
COS-7	ATCC	Cat#CRL-1651
Patas monkey skin fibroblasts	Coriell Institute for Medical Research (CIMR)	Cat#AG06254 and AG06116
Human histiocytic SU-DHL-1	ATCC	Cat#CRL-2955
Monocytic THP-1	ATCC	TIB-202
Monocytic U937	ATCC	Cat#CRL-1593.2
Kidney cell line ACHN	NCI-Frederick Cancer DCTD Tumor/Cell Line Repository	N/A
Kidney cell line CAKI-1	NCI-Frederick Cancer DCTD Tumor/Cell Line Repository	N/A
Kidney cell line786-0	NCI-Frederick Cancer DCTD Tumor/Cell Line Repository	N/A
Kidney cell line A498	NCI-Frederick Cancer DCTD Tumor/Cell Line Repository	N/A
HEK293T	ATCC	Cat#11268
Grivet kidney Vero E6	ATCC	Cat#CRL-1586
MA-104, Vero, patas monkey, human bone marrow	Takara Bio Inc.	#636643
Common chimpanzee (*Pan troglodytes*) fibroblasts	Emory University	S008886
Red-cheeked gibbon (*Nomascus gabriellae*) fibroblasts	CIMR	#PR00381
Northern white-cheeked gibbon (*Nomascus leucogenys*) fibroblasts	CIMR	#PR00712
Lar gibbon (*Hylobates lar*) fibroblasts	CIMR	#PR01131
Collared mangabey (*Cercocebus torquatus*) fibroblasts	CIMR	#PR00485
Black crested mangabey (*Lophocebus aterrimus*) fibroblasts	CIMR	#PR01215
Angolan talapoin (*Miopithecus talapoin*) fibroblasts	CIMR	#PR00716
Wolf's mona monkey (*Cercopithecus wolfi*) fibroblasts	CIMR	#PR01241
François' langur (*Trachypithecus francoisi*) fibroblasts	CIMR	#PR01099
Mantled guereza (*Colobus guereza*) fibroblasts	CIMR	#PR00980
Bolivian red howler (*Alouatta sara*) fibroblasts	CIMR	#PR00708
Oligonucleotides		
Primers for cloning nonhuman primate CD163 receptor orthologs	See Table S1 for primer sequences	N/A
CRISPR-Cas9 RNA (crRNA) targeting CD163 exon 3; AATGCGTCCAGAACCTGCAC	This study	N/A
Alt-R *trans*-activating CRISPR-Cas9 RNA (tracrRNA)	IDT	Cat#1072534

(*Continued on next page*)

Please cite this article in press as: Warren et al., Primate hemorrhagic fever-causing arteriviruses are poised for spillover to humans, Cell (2022), https://doi.org/10.1016/j.cell.2022.09.022

Continued

REAGENT or RESOURCE	SOURCE	IDENTIFIER
Recombinant DNA		
pLHCX retroviral transfer vector encoding CD163 orthologs	This study	N/A
Empty pLHCX retroviral transfer vector	Yamashita and Emerman (2004)	N/A
pCS2-mGP encoding MLV gag-pol	Yamashita and Emerman (2004)	N/A
pCMV-VSV-G (encoding vesicular stomatitis Indiana virus glycoprotein "G")	Addgene	Cat#8454
Recombinant SHFV (rSHFV)	Cai et al., 2021	N/A
Enhanced green fluorescent protein-expressing rSHFV	Cai et al., 2021	N/A
Software and algorithms		
Sequencher DNA sequence analysis software	Gene Codes Corporation	N/A
Stellaris probe designer	Biosearch Technologies	https://www.biosearchtech.com/support/tools/design-software/stellaris-probe-designer
ImageJ	Schneider et al., 2012	https://imagej.nih.gov/ij/
FlowJo v10.8.0 software	BD Life Sciences	N/A
MEGA7	Kumar et al., 2016	https://www.megasoftware.net/
MEGAX	Stecher et al., 2020	https://www.megasoftware.net/
PAL2NAL web server tool	Suyama et al., 2006	https://www.bork.embl.de/pal2nal/
Nipot v2.3	Perrière and Gouy, 1996	http://doua.prabi.fr/software/njplot
PAML4.8	Yang, 2007	N/A
Prism v9.1.0	GraphPad	N/A
QGIS v3.16.4	QGIS Geographic Information System	https://www.qgis.org/
BioRender	Created with https://Biorender.com	N/A

RESOURCE AVAILABILITY

Lead contact

Further information and requests for resources and reagents should be directed to and will be fulfilled by the lead contact, Sara L. Sawyer (ssawyer@colorado.edu).

Materials availability

There are restrictions to the availability of materials. Constructs and reagents in this study will be made available upon request, but a completed Materials Transfer Agreement may be required if there is potential for commercial application.

Data and code availability

Primate CD163 sequences have been deposited at GenBank and are publicly available as of the date of publication. Co-localization analyses (Pearson's Correlation Coefficients [PCC]) were performed using a custom MatLab script. Accession numbers and code are listed in the key resources table. Any additional information required to reanalyze the data reported in this paper is available from the lead contact upon request.

EXPERIMENTAL MODEL AND SUBJECT DETAILS

Cells

Nonhuman primate cell lines, including grivet (*C. aethiops*) embryonic kidney MA-104 Clone 1 (American Type Culture Collection [ATCC], Manassas, VA, USA, #CRL-2378.1), MA-104 subclone MARC-145 (originally provided by Dr. Kay Faaberg, U.S. Department of Agriculture [USDA], National Animal Disease Center, Ames, IA, USA), grivet kidney fibroblast COS-7 (ATCC, #CRL-1651), and patas monkey skin fibroblasts (Coriell Institute for Medical Research [CIMR], Camden, NJ, USA, #AG06254 and #AG06116) were cultured in Eagle's minimum essential medium (EMEM; ATCC, 30–2003) plus 10% fetal bovine serum (FBS; MilliporeSigma, Billerica, MA, USA, TMS-013-B) and 1X penicillin-streptomycin solution (Pen Strep; Avantor, Radnor, PA, USA, #45000-652) (complete EMEM [cEMEM]). Human histiocytic SU-DHL-1 (ATCC, #CRL-2955), monocytic THP-1 (ATCC, #TIB-202), monocytic U937 (ATCC,

#CRL-1593.2), and kidney cell lines ACHN, CAKI-1, 786-0, and A498 (obtained from the National Cancer Institute [NCI] Division of Cancer Treatment and Diagnosis [DCTD] Tumor Repository, Frederick, MD, USA) were cultured in RPMI-1640 medium (ATCC, #30–2001) plus 10% FBS and 1X Pen Strep (complete RPMI [cRPMI]). HEK293T cells (ATCC, #11268) were cultured in Dulbecco's modified Eagle's medium (DMEM; MilliporeSigma, Billerica, MA, USA, #D6429) plus 10% FBS, 1X Pen Strep, and L-glutamine (Corning Incorporated, Corning, NY, USA, #MT25005CI) (complete DMEM [cDMEM]). Grivet kidney Vero E6 cells (ATCC, #CRL-1586) were maintained in DMEM supplemented with 10% FBS. All cells were cultured at 37°C in a humidified 5% CO_2 atmosphere. Hygromycin (Corning, #30-240-CR) selection was maintained throughout culture of the following cell lines, stably transduced with retroviral vectors: MA-104 (300 μg/mL), Vero (200 μg/mL), patas monkey skin fibroblasts (50 μg/mL), 786-0 and CAKI-1 (500 μg/mL), and ACHN and A498 (250 μg/mL). The NCI-60 panel of human cell lines was handled as previously described (Cai et al., 2021).

Rhesus monkey peripheral blood mononuclear cells (PBMCs) were obtained from rhesus monkeys housed at the Keeling Center for Comparative Medicine and Research (KCCMR) in Bastrop, TX, USA. All blood collections performed for this study were approved by the MD Anderson Cancer Center Institutional Animal Care and Use Committee (OLAW assurance number A3343-01) and were performed in strict compliance with The Guide for the Care and Use of Laboratory Animals (8^{th} edition). PBMCs were seeded at >5x10^6 cells per well of a 6-well plate (CELLTREAT Scientific Products, Pepperell, MA, USA, #229105) and cultured overnight in cRPMI. The next day, cells were gently washed three times with phosphate-buffered saline (PBS; Caisson Labs, Smithfield, UT, USA, PBL01-6X500ML) to remove non-adherent lymphocytes. Macrophages were cultured from adherent cells by incubation with cRPMI supplemented with 20 ng/mL human recombinant macrophage colony-stimulating factor (M-CSF; R&D Systems, Minneapolis, MN, USA, #216-MC-010) for 5 days. Human PBMCs (Lonza, Basel, Switzerland, #4W-270A) were maintained in ImmunoCult-SF macrophage medium (STEMCELL Technologies, Vancouver, BC, Canada, #10961), supplemented with 50 ng/mL human recombinant M-CSF (CSF1; R&D Systems, 216-MC) for 6 days to allow M0 macrophage differentiation. For M1 or M2 macrophage differentiation, M0 macrophages were treated with 50 ng/mL interferon-γ (IFN-γ; R&D Systems, 285-IF) or with 10 ng/mL interleukin 4 (IL-4; MilliporeSigma, St. Louis, MO, USA, H7291), respectively, for 2 days.

Viruses

Simian hemorrhagic fever virus (SHFV) isolate LVR42-0/M6941 (ATCC, #VR-533) (Lauck et al., 2014) and cDNA-launch systems for recombinant SHFV (rSHFV) and rSHFV expressing enhanced green fluorescent protein (rSHFV-eGFP) were used as previously described (Cai et al., 2021). Briefly, for passage 0 (P0), a stock of SHFV was propagated in 1.75x10^7 MA-104 cells plated in 182-cm^2 flasks (CELLTREAT Scientific Products, #229381) using a MOI of 0.001 for 1 h at 37°C (5 mL of EMEM +2% FBS), with gentle rocking every 15 min. Inocula were then removed and replaced with 15 mL of 2% EMEM. Cell supernatants were harvested 3 days later (>80% cytopathic effect) and clarified by centrifugation at 500 x*g* for 10 min at 4°C. This P1 stock was titered by plaque assay. Briefly, MA-104 cells were seeded at 3x10^5 cells per well in 6-well plates. The following day, cell culture media were removed, virus samples were 10-fold serial-diluted in EMEM, and 300 μL of diluted samples were added to the each well of cells, followed by incubation at 37°C for 1 h, with gentle rocking every 15 min. Cells were then washed three times with PBS, and a volume of 3 mL of overlay medium (final concentration 1X phenol-free EMEM [VWR, #115-073-101] + 5% FBS + L-glutamine + 1.4% Avicel [Avicel RC-591 NF; FMC Corporation, Philadelphia, PA, USA]) was added to each well, followed by undisturbed incubation at 37°C in a humidified 5% CO_2 atmosphere for 48 h. Cells were then washed twice with PBS and fixed/stained (final concentration 10% neutral buffered formalin [MilliporeSigma, #HT501128-4L], 0.2% crystal violet [MilliporeSigma, #C3866-25G]) for 15 min. Plaques were visualized following the removal of the fix/stain solution and gentle washing. From the P1 stock, a P2 stock, which was used for all downstream experiments, was generated by exposing MA-104 cells (MOI = 0.01) as described above. rSHFV and rSHFV-eGFP were rescued from plasmids by transfection of MA-104 cells using Lipofectamine 3000 reagent (Thermo Fisher Scientific, Carlsbad, CA, USA, #L3000008). Briefly, cells were seeded at 3x10^5 cells per well in 6-well plates and, the next day, transfected with 3 μg of plasmid DNA. (Tube A contained 150 mL Opti-MEM [Thermo Fisher Scientific, #31985-070] and 4.5 μL Lipofectamine 3000; Tube B contained 150 μL Opti-MEM, 3 μg plasmid DNA, and 6 μL Lipofectamine p3000. Tube A was added to Tube B, mixed 5 min, and added dropwise to cells.) Viral titers peaked 3 days post-transfection. Ebola virus/H.sapiens-wt/GIN/2014/Makona-C05 (Baize et al., 2014; Hoenen et al., 2014) was provided by Dr. Gary Kobinger (Public Health Agency Canada, Winnipeg, MT, Canada) and propagated in Vero E6 cells as previously described (Logue et al., 2019).

METHOD DETAILS

Viral infection assays

Cells were seeded in individual wells of 6-well plates and, the next day, exposed to SHFV or Ebola virus at the indicated MOIs (see figure legends). Cells were exposed to virus in a minimal volume of media (300 μL) and incubated at 37°C for 1 h, with gentle rocking every 15 min. After incubation, cells were washed three times with PBS and then maintained in cell-type-specific media supplemented with 5% FBS. Cell supernatants were collected at indicated times post-exposure. Viral titers were determined by standard plaque assays using MA-104 cells for SHFV (Caì et al., 2015) and Vero E6 cells for Ebola virus (Logue et al., 2019). Plaque assays used overlays with final concentrations of 0.8% Tragacanth (MilliporeSigma, G1128) or 1.4% Avicel for SHFV and 1.25% Avicel for Ebola virus. At 2 days (SHFV) and 8 days (Ebola virus), overlays were removed, and plaques were counted.

Please cite this article in press as: Warren et al., Primate hemorrhagic fever-causing arteriviruses are poised for spillover to humans, Cell (2022), https://doi.org/10.1016/j.cell.2022.09.022

Western blotting

Cells were lysed in Nonidet P-40 buffer (NP-40; 150 mM sodium chloride [NaCl; Promega, Madison, WI, USA, #V4221]), 50 mM tris(hydroxymethyl)aminomethane hydrochloride [HCl] pH 7.4 [Teknova, Hollister, CA, USA, #T1075], 1% NP-40 [G-Biosciences, St. Louis, MO, USA, #DG001], 1 mM dithiothreitol [DTT] [IBI Scientific, Dubuque, IA, USA, #IB21040], 1 μL/mL Benzonase [MilliporeSigma, #E1014]), and protease inhibitor mixture (MilliporeSigma, #11873580001). Briefly, cells were detached from tissue-culture plates by trypsin EDTA; Corning, Tewksbury, MA, USA, #25-052-CI) treatment, inactivated with FBS containing media, and then pelleted (300 x*g* for 5 min) and washed once with PBS. The cells were again pelleted, resuspended in NP-40 buffer, and incubated at 4°C for 30 min on a tube revolver rotator (ThermoScientific, #88881001). Cell lysates were cleared by centrifugation at 16,000 x*g* for 15 min at 4°C. Whole-cell extracts were quantified using a bicinchoninic acid (BCA) protein assay (Thermo Fisher Scientific, #23227). Total protein (10 μg) was resolved with polyacrylamide gel electrophoresis using gels prepared with 10% Tris-glycine eXtended (TGX) stain-free acrylamide premixed gel solution (Bio-Rad, Hercules, CA, USA, #1610182) and by applying 180 V until protein-loading dye ran off the gel. Proteins were transferred to Immobilon-P PVDF membranes (MilliporeSigma, #IPVH07850) using a wet transfer apparatus (Bio-Rad Mini-Protean tetra and blotting module, #1660828EDU) set at 100 V for 1 h. Membranes were blocked in 0.1% tris-buffered saline (TBS; Research Products International [RPI], Mount Prospect, IL, USA, #T60075–4000.0) + Polysorbate 20 (TWEEN 20; Amresco, Dallas, TX, USA, #M147-1L) (TBST) + Nestle Carnation 5% nonfat dried milk (Vevey, Switzerland) for 1 h at ambient temperature. Primary antibodies (goat polyclonal anti-CD163 antibody [R&D Systems, #AF1607] and mouse monoclonal actin beta (clone 8H10D10) antibody [mAb; Cell Signaling Technology, Danvers, MA, USA, #3700S]) were diluted in TBST +5% nonfat dried milk and incubated either overnight at 4°C (anti-CD163 polyclonal antibody) or for 1 h at ambient temperature (actin beta [8H10D10] mouse mAb). After primary incubation, cells were washed three times for 5 min in TBST. Secondary antibodies—donkey anti-goat immunoglobulin G (IgG) (H + L) cross-adsorbed horseradish peroxidase (HRP) conjugate (Thermo Fisher Scientific, #A16005), anti-mouse IgG (H + L) HRP conjugate (Promega, #W402B)—were diluted in TBST +5% nonfat dried milk and incubated with the membrane for 1 h at ambient temperature. After secondary incubation, membranes were washed three times for 5 min in TBST, developed using enhanced chemiluminescent (ECL) reagent (MilliporeSigma, #GERPN2232), and imaged on a ChemiDoc Imaging System (Bio-Rad).

CRISPR-Cas9 editing of CD163

CRISPR-Cas9 RNA (crRNA) targeting grivet CD163 exon 3 (AATGCGTCCAGAACCTGCAC) was synthesized and mixed with Alt-R *trans*-activating CRISPR-Cas9 RNA (tracrRNA; Integrated DNA Technologies [IDT], Coralville, IA, USA, #1072534) to a final duplex concentration of 44 μM. RNA duplexes were heated at 95°C for 1 h and cooled to ambient temperature. Cas9 nuclease, *S. pyogenes* (New England Biolabs [NEB], Ipswich, MA, USA, NEB #M0386M) was diluted with resuspension buffer R from the Neon Transfection System Kit (Thermo Fisher Scientific, #MPK10025) to 36 μM in a 0.5-μL final solution, mixed with 0.5 μL of crRNA:tracrRNA duplex, and incubated at ambient temperature for 20 min. A total of $1x10^6$ MA-104 cells were electroporated with two 30-ms pulses of 1,150 V using the Neon Transfection System (Thermo Fisher Scientific, #MPK5000). Electroporated cells were resuspended in cEMEM and incubated for 4 days in 12-well plates (CELLTREAT Scientific Products, #229111). Genomic editing in the bulk cell populations were confirmed using the T7 endonuclease 1 (E1) assay in the Alt-R Genome Editing Detection Kit (IDT, #1075931). Single-cell clones from the CD163 exon-3-edited bulk cell population were obtained by limited dilution cloning (0.5 cells per well in 96-well plates [CELLTREAT Scientific Products, #229196]). Genomic DNA from single-cell clones was screened by the T7E1 assay to identify edited clones. CD163 knockout was confirmed by western blotting, and clone "F11" was selected for all follow-up studies. Primers flanking the crRNA target site were used to amplify a small fragment of genomic DNA using a Phusion high-fidelity polymerase chain reaction (PCR) master mix with buffer (NEB, #M0531L). A-tailed PCR fragments were then TA-cloned via sequencing with the TOPO TA Cloning Kit (Thermo Fisher Scientific, #K457501). Successful insertion of a PCR product was confirmed by blue-white screening. A total of 15 independent plasmid clones from F11-edited and parental (MA-104) cells were Sanger-sequenced (Quintara Biosciences, Cambridge, MA, USA) and sequences analyzed using Sequencher DNA sequence analysis software (Gene Codes Corporation, Ann Arbor, MI, USA). Biallelic deletions in clone F11 (ΔCACTG and ΔCA) resulted in a premature stop codon and ablation of CD163 protein expression (MA-104 ΔCD163) (Figure S1).

CD163 receptor complementation experiments

Total RNA was isolated from the following cells: MA-104, Vero, patas monkey, human bone marrow (Takara Bio Inc., Mountain View, CA, USA, #636643), common chimpanzee (*P. troglodytes*) fibroblasts (Emory University, Yerkes National Primate Research Center, Atlanta, GA, USA, S008886), red-cheeked gibbon (*Nomascus gabriellae*) fibroblasts (CIMR, #PR00381), northern white-cheeked gibbon (*Nomascus leucogenys*) fibroblasts (CIMR, #PR00712), lar gibbon (*Hylobates lar*) fibroblasts (CIMR, #PR01131), collared mangabey (*Cercocebus torquatus*) fibroblasts (CIMR, #PR00485), black crested mangabey (*Lophocebus aterrimus*) fibroblasts (CIMR, #PR01215), primary rhesus monkey PBMCs (obtained from G. K. Wilkerson, Michale E. Keeling Center for Comparative Medicine and Research, The University of Texas MD Anderson Cancer Center), Angolan talapoin (*Miopithecus talapoin*) fibroblasts (CIMR, #PR00716), wolf's mona monkey (*Cercopithecus wolfi*) fibroblasts (CIMR, #PR01241), François' langur (*Trachypithecus francoisi*) fibroblasts (CIMR, #PR01099), mantled guereza (*Colobus guereza*) fibroblasts (CIMR, #PR00980), Nancy Ma's night monkey (*Aotus nancymaae*) PBMCs (obtained from G. K. Wilkerson), and Bolivian red howler (*Alouatta sara*) fibroblasts (CIMR, #PR00708). cDNA was generated by reverse transcription with a Super-Script IV First-Strand Synthesis System (Thermo Fisher

Scientific, #18091200), and *CD163* was amplified using a Phusion high-fidelity PCR master mix with buffer (NEB, #M0531L) with gene-specific primers. *CD163* from these host cells was inserted into the Clontech pLHCX retroviral expression vector (Takara Bio Inc., #631511) using a Gibson assembly. Sequences are deposited as GenBank: MZ695198 to MZ695214.

Murine leukemia virus (MLV; *Retroviridae*: *Gammaretrovirus*) pseudotypes were generated as described previously (Warren et al., 2019a). Briefly, HEK293T cells were plated in cDMEM without antibiotics ($1x10^6$ cells per well in 6-well plates) and, the next day, transfected with 2 μg of pLHCX transfer vector (encoding CD163 receptor orthologs and hygromycin-resistance genes), 1 μg of pCS2-mGP (encoding MLV gag-pol) (Yamashita and Emerman, 2004), and 0.2 μg of pCMV-VSV-G (encoding vesicular stomatitis Indiana virus glycoprotein "G") (Addgene, Watertown, MA, USA, #8454) using a 3:1 ratio of TransIT 293 transfection reagent (Mirus Bio, Madison, WI, USA, #MIR2705) to DNA. At 48 h post-transfection, cell supernatants containing gammaretrovirus particles were collected, filtered through 0.22-μm cellulose acetate filters (GVS Life Sciences, Sanford, ME, USA, #FJ25BSCCA002AL01), and stored at −80°C. For transduction, target cells were plated at ≈15% confluence and, the next day, exposed to gammaretrovirus-containing supernatant by spinoculation at 1,200 x*g* for 75 min in the presence of 3 μg/mL polybrene hexadimethrine bromide (MilliporeSigma, 107,689-10G). The following day, media were replaced with fresh media and, 48 h later, cells were placed in media containing hygromycin throughout their time in culture.

CD163 detection by flow cytometry

For each cell line analyzed, $1x10^5$ cells were added to three wells of a 96-well v-bottom plate. Each well was handled as follows: well #1, unstained control; well #2, surface stain only; well #3, intracellular stain only. The cells were pelleted at 250 x*g* for 5 min, washed once with PBS, and then proceeded to surface staining. For surface stains, each well was handled as follows: wells #1 and #3, cells were resuspended in 50 μL fluorescence-activated cell sorting (FACS) buffer (PBS +2% FBS +1 mM EDTA); well #2, cells were re-suspended in 50 μL FACS buffer +1:25 dilution of APC-conjugated CD163 antibody (clone GHI/61, BioLegend, #333609). The cells were incubated at 4°C for 30 min in the dark and then washed three times with FACS buffer. The cells were then resuspended in 200 μL of fixation/permeabilization solution (BD Cytofix/cytoperm kit, #554714) and then incubated at 4°C for 20 min in the dark. The cells were then washed two times in 200 μL of perm/wash buffer (BD Cytofix/cytoperm kit) and then proceeded to intracellular staining. For intracellular stains, each well was handled as follows: wells #1 and #2, cells were resuspended in 50 μL of perm/wash buffer; well #3, cells were resuspended in 50 μL of perm/wash buffer +1:25 dilution of APC-conjugated CD163 antibody (clone GHI/61, BioLegend). The cells were incubated at 4°C for 30 min in the dark and then washed three times with perm/wash buffer. After the final wash, the cells were resuspended in FACS buffer and analyzed by flow cytometry.

Design and labeling of smFISH probes

A total of 48 probes (20 nucleotides in length, 2 nucleotides minimum spacing) were designed antisense to SHFV ORF1a using the Stellaris probe designer (Biosearch Technologies, Petaluma, CA, USA, https://www.biosearchtech.com/support/tools/design-software/stellaris-probe-designer). Probes were then ordered according to a 96-well plate layout from IDT and directly conjugated with 2′,3′-dideoxyuridine-5′-triphosphate (ddUTP) and labeled with fluorescent dyes by combining the following reagents and incubating overnight: 10 μL 5X terminal deoxynucleotidyl transferase (TdT) buffer, 1 μL TdT (Thermo Fisher Scientific, #EP0161), 5 μL probe mix (10 μL of each DNA oligo were pooled, and then 5 μL of these mixtures were used in the labeling reaction), and 3 μL 5-propargylamino-ddUTP ATTO 633 (Jena Bioscience, Jena, Thuringia, Germany, #NU-1619-633). Probes were incubated for 8 h at 37°C in the dark. Then, an additional volume of 0.75 μL TdT was added and mixed, and incubation was continued overnight (≈24 h total). To precipitate probes, 50 μL of 3 M sodium acetate (NaOAc; Amresco, #E498-200ML) and 400 μL of 100% cold ethanol (EtOH; Thermo Fisher Scientific, # 04-355-223) were added to each reaction, and then the samples were stored at −20°C for 30 min. Oligos were pelleted by centrifugation at 16,000 x*g* for 15 min at 4°C, washed two times with 70% cold EtOH, resuspended in nuclease-free water (IBI Scientific, # IB42201), aliquoted into single-use tubes, and stored at −80°C.

Sequential immunofluorescence and smFISH

Wild-type MA-104 and MA-104 ΔCD163 cells were seeded onto acid-etched coverslips in 6-well plates at ≈80% confluency ($2.1x10^5$ cells per well). Primary rhesus monkey macrophages (Figures 4C and 4D) were seeded at $1x10^5$ cells per well with 1 μg/mL poly-L-lysine-coated (MilliporeSigma, #P8920) for 1 h at 37°C on glass plates (DOT Scientific, Burton, MI, USA, #MGB096). Cells were exposed to SHFV (MOI = 10) or mock-exposed for the indicated duration. Following exposure, cells were washed three times with PBS, fixed with paraformaldehyde (PFA; VWR, #100504-85) in PBS (4% final concentration) undisturbed for 10 min at ambient temperature. Following two PBS washes, cells were permeabilized using 0.1% Triton X-100 (VWR, # JTX198-5) for 5 min at ambient temperature. Permeabilization solution was removed, and cells were washed once with PBS and then incubated with primary antibodies—mouse purified monoclonal anti-CD163 antibody clone GHI/61 (Biolegend, San Diego, CA, USA, #333602) and/or rabbit polyclonal anti-occludin antibody (Thermo Fisher Scientific, #71-150-0)—for 1 h at ambient temperature. Following three 10-min PBS washes, cells were incubated with Alexa-Fluor-labeled secondary antibodies—goat anti-mouse IgG AF488+ (Invitrogen, Waltham, MA, USA, #A32723) and/or goat anti-rabbit IgG AF546 (Invitrogen, #A11010)—for 1 h at ambient temperature. Cells were then washed three times with PBS for 10 min each and refixed as detailed above.

For smFISH, cells were washed twice with PBS and once with 1X Wash Buffer A (Biosearch Technologies, #SMF-WA1-60) following fixation. Cells were incubated with hybridization buffer (Biosearch Technologies, #SMF-HB1-10), containing smFISH

Please cite this article in press as: Warren et al., Primate hemorrhagic fever-causing arteriviruses are poised for spillover to humans, Cell (2022), https://doi.org/10.1016/j.cell.2022.09.022

probes (1-μL probe per 100-μL hybridization reaction), at 37°C for 16 h in the dark. Cells were then incubated with Wash Buffer A at 37°C for 30 min. Then, macrophages (plated on glass plates) were counterstained with Hoechst 33,342 dye for DNA and nuclei (Invitrogen, #H3570) at a 1:5,000 dilution in Wash Buffer A for 15 min at 37°C, while cell lines continued processing (on glass coverslips). Staining buffer was removed, the cells were washed once with Wash Buffer B (Biosearch Technologies, #SMF-WB1-20) for 5 min, and then either stored in PBS at 4°C (macrophages) or mounted onto glass slides (cell lines) using Prolong Gold Antifade Mountant with 4′,6-diamidino-2-phenylindole (DAPI; Thermo Fisher Scientific, #P36941). Mounted coverslips were cured for 2 days at ambient temperature prior to imaging.

Microscopy and image processing

Laser scanning confocal microscopy images were acquired on a A1R laser scanning confocal microscope (Nikon Metrology, Brighton, MI, USA) using a 1.45 NA 100x oil objective, 405/488/561/640 laser lines, and photomultiplier tube detectors. Z-stacks were collected at Nyquist resolution through the volume of several cells in each condition, and the acquisition parameters were adjusted to optimize the signal-to-noise ratio for each image and condition. Image processing was performed using ImageJ analysis software (Schneider et al., 2012) (National Institutes of Health [NIH], Bethesda, MD, USA). Maximum-intensity projections are shown for representative images in Figures 3A, 3B, and 3C; single z-planes are shown for orthogonal images in Figure 3E. Brightness and contrast were adjusted, when needed, to display the full dynamic range of each image. Pearson's correlation coefficient (PCC) analysis (Figure 3D) was performed with a custom MATLAB script that was adapted from (Peters and Garcea, 2020) and based on the image analysis practices outlined in (Aaron et al., 2018). Briefly, a percentile-based threshold was applied to each channel in each image. A PCC value was calculated for all co-localizing pixels in each pair of channels, reflecting the relative co-occurrence of the corresponding fluorescent signals throughout the z stack image. For imaging rSHFV-eGFP-infected cells, cells were fixed with 10% neutral buffered formalin (VWR, #16004-128) and stained with Hoechst 33,342 (Thermo Fisher Scientific, #H3570) 3 days after virus exposure. Images were taken by Operetta CLS (PerkinElmer, Dumfries, VA, USA).

FISH-flow

Wild-type MA-104 or MA-104 ΔCD163 cells were either (1) exposed to SHFV (Figure S4) or (2) transfected with SHFV-encoding plasmids (Figure S3). At the indicated times following exposure/transfection, cell-culture media was removed, and the cells were washed three times with PBS. Cells were detached with trypsin, inactivated with FBS-containing media, and then transferred to individual wells of a 96-well v-bottom plate (NEST Scientific, Wuxi, China, #701211). Cells were washed once with PBS and then fixed with 4% PFA (VWR, #100504-858) for 10 min at ambient temperature. Cells were pelleted at 500 *xg* for 5 min, washed three times with PBS, and then permeabilized with cold 70% EtOH for at least 1 h at 4°C. Cells were pelleted, washed once with Wash Buffer A, and resuspended in 50 μL of hybridization buffer containing probe (one 0.5-μL probe per 50-μL reaction). The plate was incubated in the dark at 37°C for 16 h. After incubation, 150 μL of Wash Buffer A were added. Cells were pelleted, resuspended in 200 μL of Wash Buffer A, and incubated in the dark at 37°C for 30 min. After incubation, cells were pelleted and resuspended in Wash Buffer B. Cells were pelleted once more and resuspended in FACS buffer (MilliporeSigma, #324506-100ML), comprised of PBS +2% FBS +1 mM EDTA. Samples were analyzed on an Accuri C6 Cytometer (BD, East Rutherford, NJ, USA). At least 50,000 live cell events were collected following singlet discrimination. Data was analyzed with FlowJo v10.8.0 (Becton, Dickinson and Company, Franklin Lakes, NJ, USA).

Phylogenetic analysis

Sequences of 33 representative nidovirals were downloaded from a previously published analysis (Nga et al., 2011). Basic Local Alignment Search Tool (BLAST) searches using RNA-directed RNA polymerase (RdRp) and helicase domains from SHFV were queried against simian arteriviruses, and multiple sequence alignments (using the Clustal tool in Molecular Evolutionary Genetics Analysis Version 7 [MEGA7] software with default parameters (Kumar et al., 2016)) were generated to identify and parse homologous regions for all simian arteriviruses. Phylogenetic relationships were inferred using the maximum-likelihood method based on the JTT matrix-based model (Jones et al., 1992). The tree with the highest log likelihood (−30036.74) is shown. Initial tree(s) for the heuristic search were obtained automatically by applying Neighbor-Join and BioNJ algorithms using default parameters in MEGA7 (Kumar et al., 2016) to a matrix of pairwise distances estimated using a JTT model and then selecting the topology with superior log likelihood value. The tree is drawn to scale, with branch lengths measured in the number of substitutions per site. The analysis involved 44 amino acid sequences with a total of 746 positions in the final dataset. Bootstrap analysis was used to test the robustness of the tree topology (100 resamplings).

Evolutionary analysis of positive selection

Gene sequences (Figure S5) were aligned to the longest human isoform in MEGA Version 10 (MEGA X) for MacOS (Stecher et al., 2020) using the ClustalW alignment tool. Multiple sequence alignments were visually inspected, duplicate gene sequences were removed, and the gene isoform from each animal that best aligned to the human reference was retained for further analysis. Terminal stop codons were removed and aligned DNA and protein sequences were exported as fasta files. Codon alignments were generated using the PAL2NAL web server tool (Suyama et al., 2006). Species cladograms for use in the PAML4.8 software package (Yang, 2007) were constructed following the species-rank phylogenetic relatedness of primates (Perelman et al., 2011). Cladograms were

generated using Newick-formatted files and viewed with Njplot version 2.3 (Perrière and Gouy, 1996). Codon alignments and unrooted species cladograms were used as input files for analysis of positive selection using PAML4.8. To detect selection, multiple sequence alignments were fit to the NSites models M7 (neutral model, codon values of dN/dS fit to a beta distribution bounded by 0 and 1), M8a (neutral model, similar to M7 but with an extra codon class fixed at a dN/dS value equal to 1), and M8 (positive selection model, similar to M8a but with the extra codon class allowed to have a dN/dS greater than 1). A likelihood ratio test was performed to assess whether the model of positive selection (M8) yielded a significantly better fit to the data compared to null models (model comparisons M7 versus M8 and M8a versus M8). Posterior probabilities (Bayes Empirical Bayes analysis) were assigned to individual codons with dN/dS values greater than 1.

African nonhuman primate range data

Range data of simian arterivirus-infected African nonhuman primates (Figure 1C) were downloaded from the International Union for Conservation of Nature (IUCN) Red List (https://iucnredlist.org/) as shapefiles and visualized in QGIS (v3.16.4) (https://www.qgis.org/). Cartoon schematics were created using https://biorender.com/.

QUANTIFICATION AND STATISTICAL ANALYSIS

Correlations between viral RNA and cellular markers by microscopy were determined using Pearson's correlation analysis of the laser scanning confocal microscopy images. Data are presented as mean ± SEM unless otherwise indicated in figure legends. Experimental repeats are indicated in figure legends. Differences in means were considered significantly different at $p < 0.05$. Significance levels are: * $p < 0.05$; ** $p < 0.01$; *** $p < 0.001$; **** $p < 0.0001$; n.s., non-significant. Analyses were performed using Prism version 9.1.0 (GraphPad, La Jolla, CA, USA).

Supplemental figures

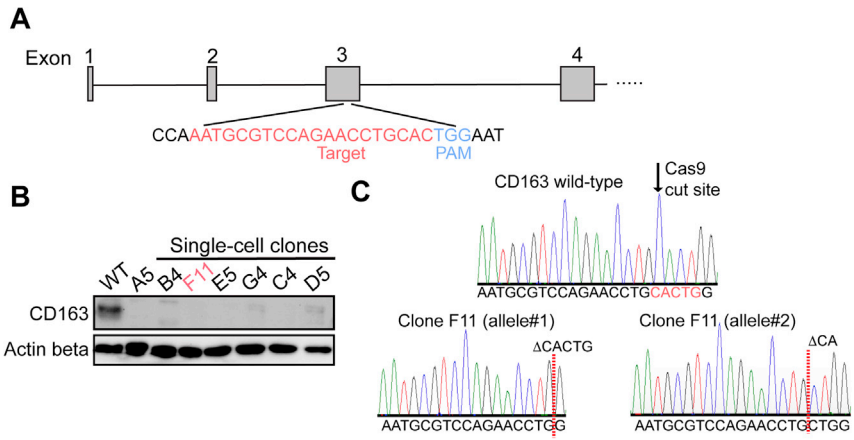

Figure S1. Strategy and confirmation of CD163 knockout in MA-104 cells, related to Figure 2

(A) Genomic organization of the first four exons of the *CD163* gene. The sequence in exon 3 that was targeted by the guide RNA is shown in red, with the protospacer adjacent motif (PAM) sequence in blue. (B) Western blotting of CD163 receptor expression in wild-type and single-cell knockout clones generated by the limiting dilution method. (C) CRISPR/Cas9 base editing was confirmed by Sanger sequencing of multiple cloned polymerase chain reaction (PCR) amplicons from wild-type and clone F11 ΔCD163 cell lines.

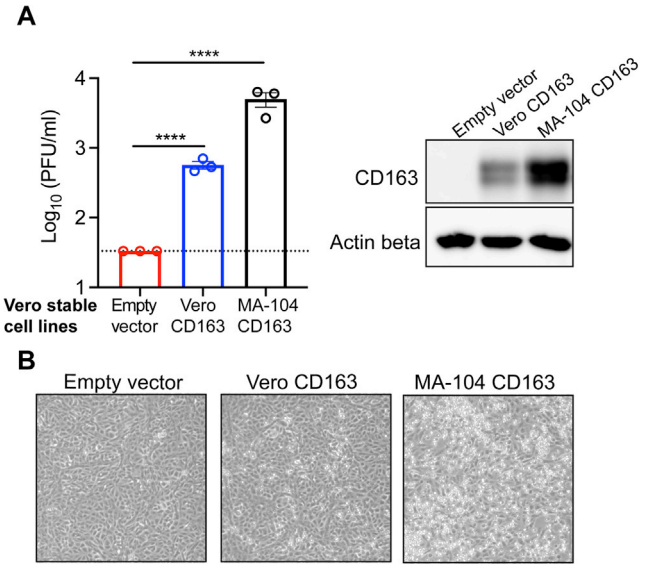

Figure S2. Restoration of CD163 expression in CD163^{null} Vero cells is sufficient for restoring infectious SHFV particle production, related to Figure 2

(A) The *CD163* gene from Vero and MA-104 cells was cloned into retroviral expression vectors. Vero cells were transduced with CD163-encoding gammaretrovirus derived from Vero or MA-104 cells, or empty vector, and stable cell lines were generated following antibiotic selection. Stable cell lines were exposed to SHFV (MOI = 3) and cell supernatant was harvested 24 h post-exposure. Viral titers were assessed by plaque assay, and the data show the mean +/− SEM(SEM; one-way ANOVA with Dunnett's post-test ****$P < 0.0001$) from three independent experiments, with one replicate per experiment. Dotted lines represent the limit of detection for the assay. Lysates from cells were probed for expression of CD163 by western blotting. Actin beta served as a protein loading control. (B) Bright-field images of cells in panel A taken 24 h post-exposure to virus. SHFV, simian hemorrhagic fever virus.

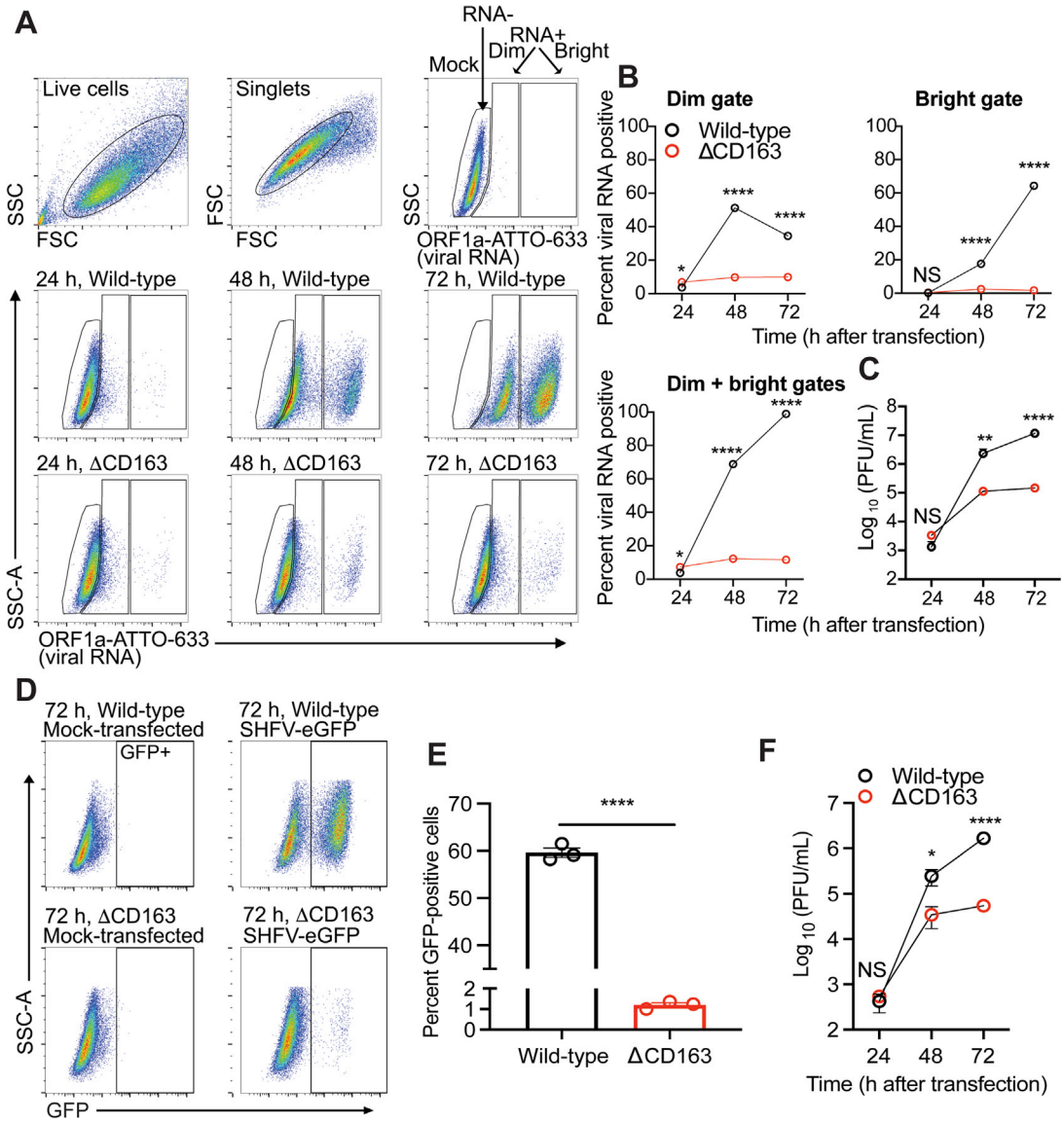

Figure S3. Transfection of wild-type rSHFV or cDNA launch plasmid encoding rSHFV-eGFP bypasses the requirement for CD163, related to Figures 2 and 3

A newly developed flow cytometric assay based on fluorescence *in situ* hybridization ("FISH-Flow") was used to enumerate the percentage of cells containing intracellular SHFV genomic RNA. (A) SHFV exposure of ΔCD163 cells did not yield progeny SHFV (Figure 2B), but cells transfected with rSHFV-eGFP-encoding plasmid resulted in sustained virus RNA within cells. Cells were either mock-transfected (top) or transfected with rSHFV-eGFP-encoding plasmid (control, middle; ΔCD163, bottom) and analyzed at 24, 48, and 72 h post-transfection. All flow cytometric events were gated on FSC x SSC properties, followed by singlet discrimination. FISH-Flow analysis quantified probe fluorescence for ATTO-633-conjugated SHFV ORF1a (viral RNA), relative to side scatter area (SSC-A). Data are representative of two independent experiments. (B) Percentage of viral RNA-positive cells in the dim (top left), bright (top right), and both dim and bright gates (bottom) for control (black circles) and ΔCD163 (red circles)-transfected cells. (C) Viral titers from cell supernatants transfected with rSHFV were assessed by plaque assay; the data show the mean +/− SEM from two independent transfection experiments. (D) Confirmation of the importance of CD163 during virion entry using rSHFV-eGFP. Flow cytometric analysis of eGFP-fluorescence in rSHFV-eGFP-encoding plasmid-transfected cells analyzed 72 h post-transfection. Cells were gated as described in panel A, and mock-transfected cells were used to denote the GFP + gate. Data are representative of three independent experiments. (E) Percentage of eGFP-positive cells enumerated from panel D. (F) Viral titers were assessed by plaque assay from supernatants of cells transfected with rSHFV-eGFP; the data show the mean ± SEM from three independent transfection experiments. (B, C, F) Two-way ANOVA with Sidak's post-test of control compared to ΔCD163 cells (*$P < 0.05$, **$P < 0.01$, ****$P < 0.0001$). (E) Unpaired two-tailed t-test (****$P < 0.0001$). In contrast to control cells, rSHFV was unable to seed a spreading infection in cells lacking CD163. Similar findings were demonstrated for rSHFV-eGFP, as examined by eGFP flow cytometry and plaque assays. SHFV, simian hemorrhagic fever virus; rSHFV, recombinant SHFV; cDNA, complementary DNA; rSHFV-eGFP, rSHFV expressing enhanced green fluorescent protein.

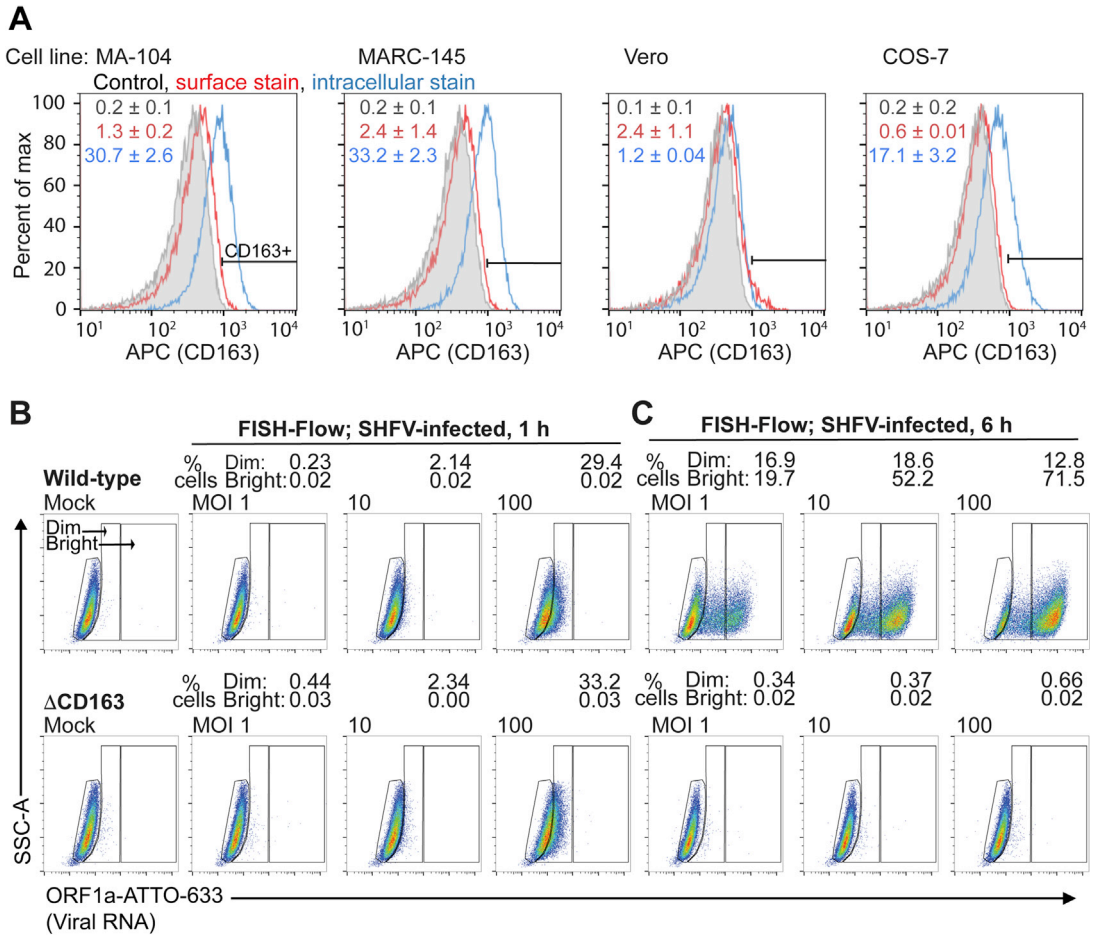

Figure S4. SHFV infects MA-104 cells lacking CD163 but cannot spread to new cells, related to Figure 3

(A) CD163 expression in the indicated cell lines following cell surface staining (red) and intracellular staining (blue) was measured by flow cytometry. Shaded histograms are from unstained cells and denote the CD163-negative population. The CD163-positive region is indicated by a black line from the 10^3 to the 10^4 decade, and the percentage of cells within this decade was enumerated for all cell lines. Shown are representative histograms. Values indicate the mean percentage of CD163-expressing cells +/− SEM from two independent experiments. APC, Allophycocyanin. Both wild-type and matched ΔCD163 cells were exposed to SFHV and analyzed by a flow cytometric assay based on fluorescence *in situ* hybridization (FISH-Flow) (B) 1 h or (C) 6 h later. Samples were either mock-exposed or SHFV-exposed at increasing multiplicities of infection (MOIs; 1, 10, or 100 PFU per cell). All flow-cytometric events were gated on FSC x SSC properties, followed by singlet discrimination. A total of at least 50,000 events was collected within the singlet gate. FISH-Flow analysis quantified probe fluorescence for ATTO-633-conjugated SHFV ORF1a (viral RNA), relative to side scatter area (SSC-A). The percentage of RNA-positive cells falling into the dim or bright gates is denoted above the graphs. (B) At 1 h, an MOI-dependent shift of both wild-type and ΔCD163 cells was observed into a dim RNA-positive gate, suggesting that SHFV indeed has mechanisms to enter cells in the absence of CD163. In a parallel experiment, the cells were harvested 6 h post-virus-exposure (when first evidence of cytopathic effects were noted). (C) In wild-type cells, an MOI-dependent shift in viral RNA-positive cells from the dim to bright gates was observed, likely indicating robust viral RNA amplification. However, viral RNA-positive ΔCD163 cells were no longer detected, indicating viral RNA clearance. SHFV, simian hemorrhagic fever virus.

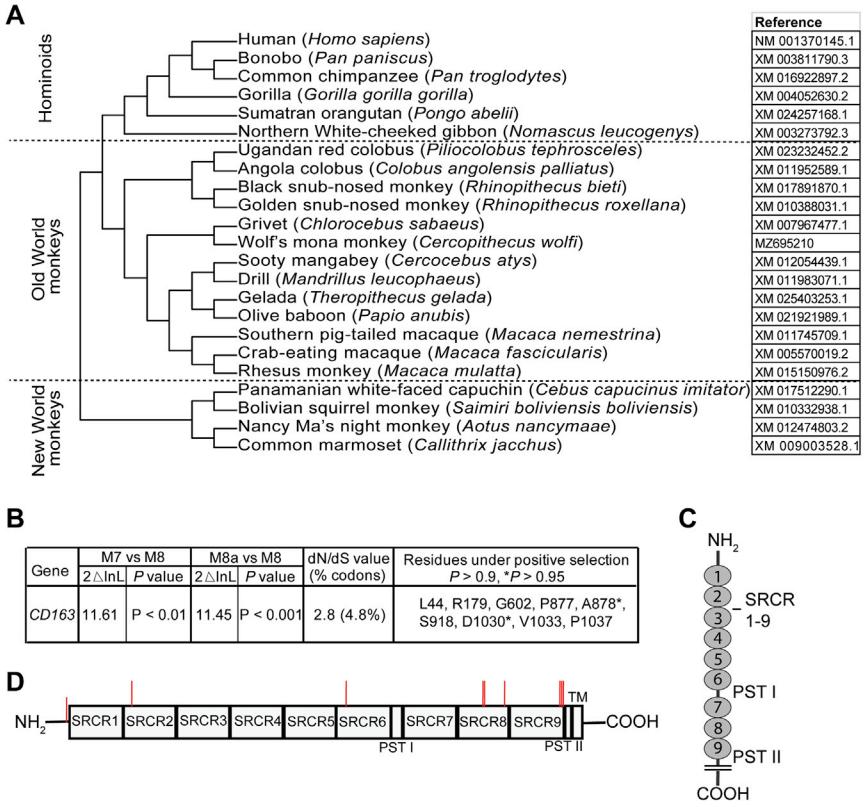

B

Gene	M7 vs M8		M8a vs M8		dN/dS value	Residues under positive selection
	2△lnL	*P* value	2△lnL	*P* value	(% codons)	*P* > 0.9, **P* > 0.95
CD163	11.61	P < 0.01	11.45	P < 0.001	2.8 (4.8%)	L44, R179, G602, P877, A878*, S918, D1030*, V1033, P1037

Figure S5. CD163 bears signatures of positive natural selection, related to Figure 4

To detect evidence of positive (diversifying) selection in primate *CD163,* testing for site-specific selective pressures was performed using the phylogenetic analysis using maximum-likelihood (PAML) program (Yang, 2007). (A) Cladogram of primates used in this analysis with corresponding National Center for Biotechnology Information (NCBI) sequence identifiers. (B) Positive selection among amino acid sites was tested by two model comparisons, M7 vs. M8 and M8a vs. M8. In each of these comparisons, the null models (M7 and M8a, respectively) do not allow for sites under positive selection, whereas the alternative model (M8) does. Twice the difference in the natural logs of the likelihoods (2 ΔlnL) is shown for each model comparison. A statistical comparison of the log likelihood ratios from these models was highly significant ($P < 0.01$), rejecting the null models in favor of the positive selection model. Residues shown correspond to codons assigned to the class with a dN/dS ratio of >1 in M8 ($P > 0.90$) by Bayes empirical Bayes (BEB) analysis. (C) Illustration of the CD163 receptor, showing the extracellular scavenger receptor cysteine-rich (SRCR domains 1–9), domains rich with proline serine threonine (PST) I and II, and the short cytoplasmic tail. The N-terminus (amine terminus; NH_2) and C-terminus (carboxyl terminus; COOH) denote the beginning and end of the protein polypeptide chain, respectively. (D) Linear domain diagram of the CD163 receptor with red tick marks denoting the location of codons under positive selection. Seven of the nine selected residues map to SRCR domains 6–9, an area that contains regions important to arterivirus infection (Gorp et al., 2010).

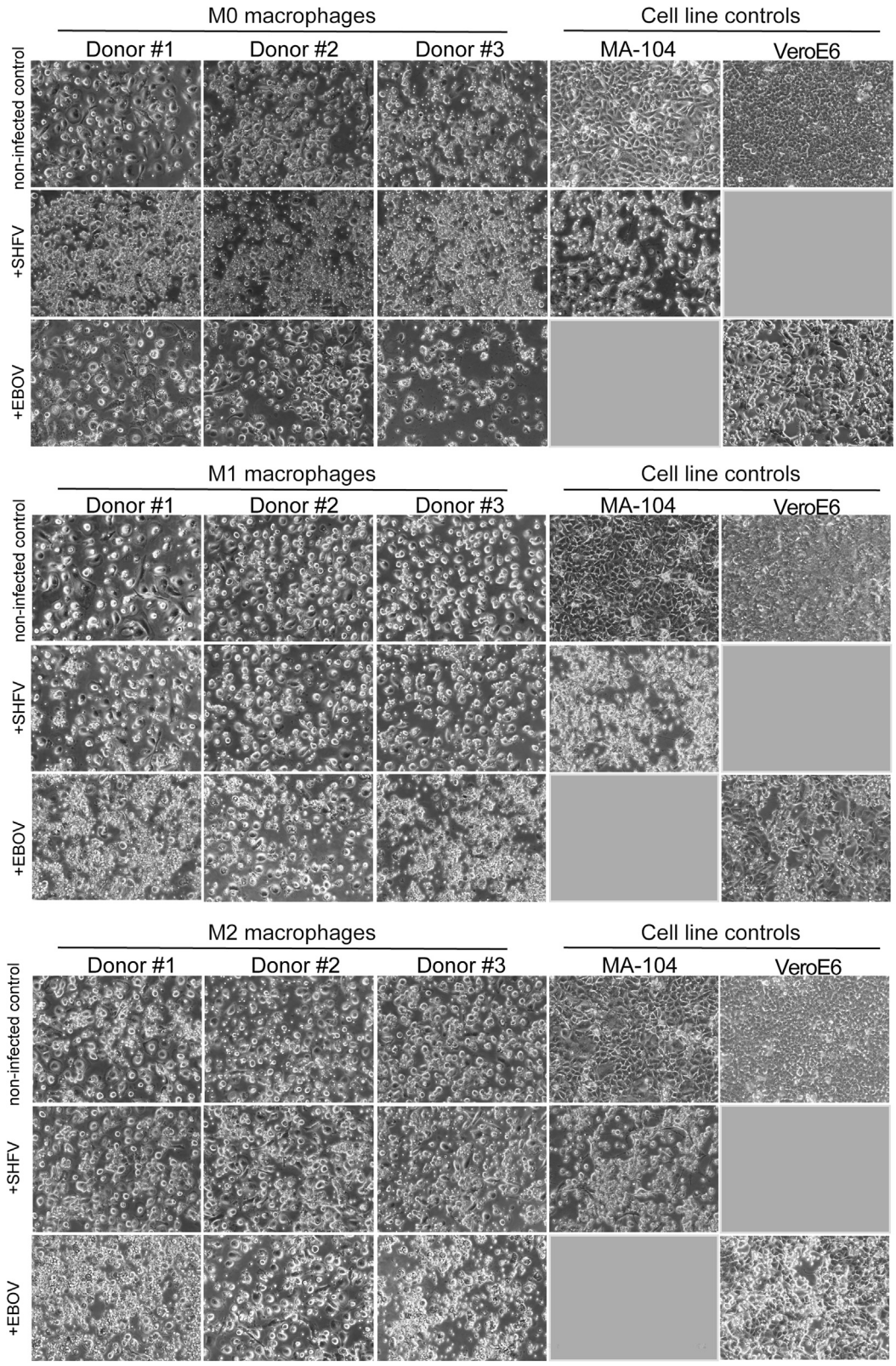

(legend on next page)

Figure S6. Human macrophages are microscopically healthy following SHFV, but not Ebola virus, exposure, related to Figure 5

Monocytes were isolated from human peripheral blood mononuclear cells (PBMCs; n = 3 donors) and differentiated into M0 macrophages. M0 macrophages were further polarized into M1 or M2 subsets using IFN-γ or IL-4, respectively. Monocyte-derived macrophages were exposed to SHFV (MOI = 3) or Ebola virus (MOI = 3). Exposures of MA-104 and Vero E6 cells served as cell line controls for SHFV and Ebola virus, respectively. Representative bright field images of cells were taken at 72 h post-exposure at 20X magnification. SHFV, simian hemorrhagic fever virus; EBOV, Ebola virus.

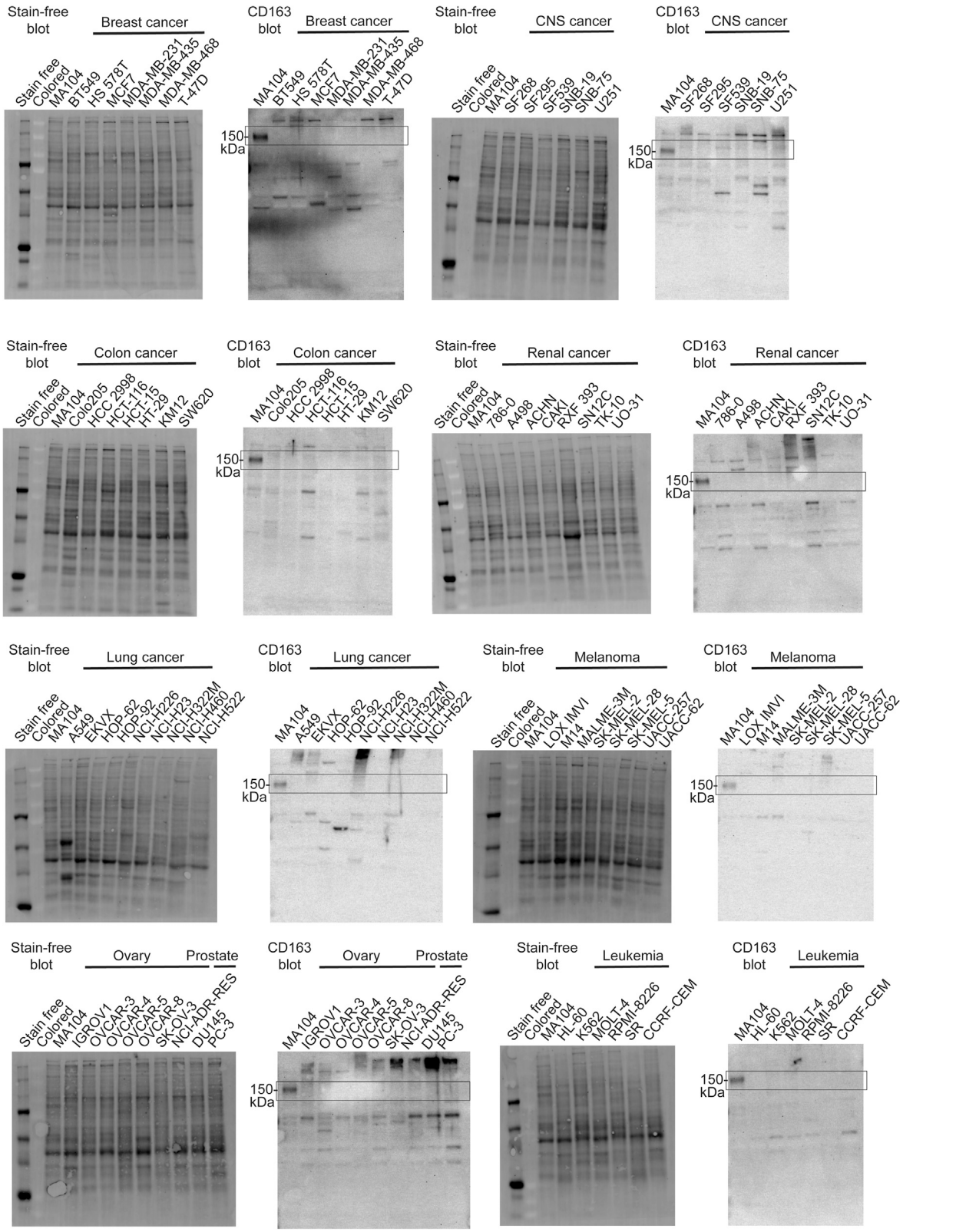

(legend on next page)

Figure S7. CD163 protein expression is undetectable in all cell lines of the human NCI-60 cancer panel, related to Figure 6

Expression of CD163 in grivet MA-104 cells permissive to simian hemorrhagic fever virus (SHFV) compared to cells of the human NCI-60 cancer panel by western blotting. A single 150-kDa band at the expected molecular weight (boxed insert in "CD163 blot") for CD163 is denoted. Equivalent protein loading was ensured by total protein stain following transfer to a PVDF membrane ("stain-free blot"). All blots shown were photographed for a maximum of 5 min. CNS, central nervous system.